Journal of Toxicology and Environmental Health, Part A: Current Issues
Publication details, including instructions for authors and subscription information:
http://www.tandfonline.com/loi/uteh20

Modeling Approaches for Estimating the Dosimetry of Inhaled Toxicants in Children

Gary L. Ginsberg [a] , Bahman Asgharian [b] , Julia S. Kimbell [b] , James S. Ultman [c] & Annie M. Jarabek [d]

[a] Connecticut Department of Public Health, Hartford, CT, USA

[b] The Hamner Institutes for Health Sciences, Research Triangle Park, NC, U.S.A

[c] Pennsylvania State University, University Park, PA, USA

[d] National Center for Environmental Assessment and National Health and Environmental Effects Research Laboratory U.S. EPA, Research Triangle Park, NC, U.S.A

Version of record first published: 20 Dec 2007

To cite this article: Gary L. Ginsberg, Bahman Asgharian, Julia S. Kimbell, James S. Ultman & Annie M. Jarabek (2007): Modeling Approaches for Estimating the Dosimetry of Inhaled Toxicants in Children, Journal of Toxicology and Environmental Health, Part A: Current Issues, 71:3, 166-195

To link to this article: http://dx.doi.org/10.1080/15287390701597889

Journal of Toxicology and Environmental Health, Part A, 71: 166–195, 2008

ISSN: 1528-7394 print / 1087-2620 online
DOI: 10.1080/15287390701597889

Taylor & Francis
Taylor & Francis Group

Modeling Approaches for Estimating the Dosimetry of Inhaled Toxicants in Children

Gary L. Ginsberg[1], Bahman Asgharian[2], Julia S. Kimbell[2], James S. Ultman[3], and Annie M. Jarabek[4]

[1]*Connecticut Department of Public Health, Hartford, CT,* [2]*The Hamner Institutes for Health Sciences, Research Triangle Park, NC, U.S.A,* [3]*Pennsylvania State University, University Park, PA, and* [4]*National Center for Environmental Assessment and National Health and Environmental Effects Research Laboratory U.S. EPA, Research Triangle Park, NC, U.S.A*

Risk assessment of inhaled toxicants has typically focused upon adults, with modeling used to extrapolate dosimetry and risks from lab animals to humans. However, behavioral factors such as time spent playing outdoors may lead to more exposure to inhaled toxicants in children. Depending on the inhaled agent and the age and size of the child, children may receive a greater internal dose than adults because of greater ventilation rate per body weight or lung surface area, or metabolic differences may result in different tissue burdens. Thus, modeling techniques need to be adapted to children in order to estimate inhaled dose and risk in this potentially susceptible life stage. This paper summarizes a series of inhalation dosimetry presentations from the U.S. EPA's Workshop on Inhalation Risk Assessment in Children held on June 8–9, 2006 in Washington, DC. These presentations demonstrate how existing default models for particles and gases may be adapted for children, and how more advanced modeling of toxicant deposition and interaction in respiratory airways takes into account children's anatomy and physiology. These modeling efforts identify child-adult dosimetry differences in respiratory tract regions that may have implications for children's vulnerability to inhaled toxicants. A decision framework is discussed that considers these different approaches and modeling structures including assessment of parameter values, supporting data, reliability, and selection of dose metrics.

INTRODUCTION

The level of injury produced by inhaled toxicants depends upon the dose received by the lungs and internal organs. This dose is a function of numerous factors including (1) type of inhaled material, (2) region of the respiratory tract affected, (3) individual's ventilation rate, (4) type of breathing (oral vs. nasal), and (5) anatomical features such as airway diameter, branching pattern and regional surface area (USEPA, 1994). A number of these host-specific factors (e.g., airway architecture and ventilation rate) vary with age such that children generally inhale more air per body weight and respiratory tract surface area than adults (USEPA, 2002; Foos, et al., 2007). This can lead to child-adult differences in delivered dose, elimination, and toxicity. Models that estimate children's dosimetry are needed in assessing children's inhalation exposure and risk. Such efforts may point out whether higher delivered dose is a reason that children appear to be particularly sensitive to inhaled particles (Schwartz, 2004; Ha, et al., 2003) and gases (Gent, et al., 2003).

While our main focus is upon dosimetry in the respiratory tract, it is important to recognize that some inhaled gases are not extracted into tissues of the nose or conducting airways but penetrate distally to the pulmonary region where systemic absorption takes place. Due to greater ventilation rate and immature metabolism in young children (Makri et al., 2004), there may also be child-adult dosimetry differences for inhaled toxicants that are systemically absorbed (Nong, et al., 2006). Therefore, both local and systemic dosimetry may need to be simulated in children's inhalation models depending upon the nature of the inhaled material.

Fortunately, there are a variety of models available to simulate inhalation dosimetry of particles and gases and these models are generally adaptable to children's physiologic and anatomical parameters. However, due to data gaps for critical parameters such as airway architecture, available models are limited in detail and may miss important local areas of high deposition that may differ across age groups. Further, there are few datasets for the calibration or verification of children's models, particularly for young children where child-adult differences are expected to be greatest.

This paper summarizes presentations from an inhalation dosimetry session that was part of a two-day workshop on children's inhalation exposures and risks sponsored by the U.S.

Address correspondence to Gary L. Ginberg Connecticut Dept. of Public Health, 410 Capitol Ave., Mail Stop 11 CHA, Hartford, CT 06134; Phone: 860-509-7750; Fax: 860-509-7785. E-mail: gary.ginsberg@po. state.ct.us

EPA (June 8 – 9, 2006, Washington, DC). The session described research to adjust default modeling approaches for children's inhalation parameters, included a discussion of more detailed models for inhaled particles and gases and a presentation of a decision analytical framework for evaluating children's dosimetry models. The presentations are summarized in Table 1 and in the following sections. An introductory section describing general principles of respiratory dosimetry as affected by anatomical factors and the type of inhaled material is included. These principles provided the scientific basis and background for the workshop.

REGIONS TARGETED BY INHALED TOXICANTS

Figure 1 shows a simplified representation of the respiratory tract divided into broad regions that receive deposition from different categories of inhaled materials. These regions have been demarcated based on major differences in size, structure, and function (U.S. EPA, 1994). These differences in turn exert dramatic effects on dosimetry in each region. The most proximal region, the upper respiratory tract, also referred to as the extra-thoracic region (ET), consists of the nose, larynx and pharynx. Large particles having a mass median aerodynamic diameter (MMAD) of ≥ 10 μm impact on the walls and bifurcation points of the ET (U.S. EPA, 1994). This region is coated by mucus which protects the epithelium from gas absorption (and can alternatively result in toxic reaction products) or transport deposited particles out of the respiratory tract. This latter pathway results in secondary absorption in the GI tract. Smaller particles ranging in size from 2.5 to 10 μm penetrate beyond the ET to the trachea and bronchi, referred to as the tracheobronchial (TB) region (U.S. EPA, 1994). These conducting airways decrease in diameter and have an increasing number of branch points with increasing distance from the trachea. There are approximately 15 branch points or generations between the trachea and the pulmonary region, with the mucus coating progressively thinning with distance. Particles depositing in this region are typically cleared by physical dissolution or mucociliary action, or are transported to the interstitium via the lymphatics (ICRP, 1994). The relative contribution of these various clearance or defense mechanisms depends on particle size and distribution which also influences the location of initial deposition. For example, mucociliary clearance is less efficient in the deep bronchioles where dissolution and lymphatic clearance dominate. As described below, some models of respiratory tract deposition divide the human TB region into the upper bronchi extending to generation 8 (BB) and the lower bronchioles (bb) that range below generation 8 to the terminal bronchioles. These bronchioles have the capacity for gas exchange with the blood, but most of this exchange occurs in alveoli in the pulmonary (PU) region. Particles below 2.5 μm and above the nano-size range are most able to penetrate to the PU region (Cheng, 2003). Clearance in this region may be by macrophage ingestion, lymphatic drainage, or in some cases dissolution. Particles have greater potential to induce adverse effects in this region due to longer retention and because macrophage ingestion may initiate an inflammatory reaction. The size cut points for deposition in the various respiratory regions are not absolute but provide a reasonable framework for understanding particle dosimetry.

This outline of respiratory architecture is also useful for describing where reactive (Categories 1 and 2) and nonreactive (Category 3) gases are extracted from the air stream (Figure 2). In 1994, the EPA introduced a categorization

TABLE 1
Children's Inhalation Dosimetry Workshop Presentations

Speaker	Title	Material covered
Ginsberg	Application of default models to evaluate child/adult differences in regional and systemic dose	Default models for inhaled particles and gases run for 3-mo-old children and adults; includes regional dosimetry in lungs and systemic dosimetry for Category 3 gases as defined in U.S. EPA (1994).
Ashgarian	Particule dosimetry modeling in the lungs of children	Multipathway lobar model run for ages 3 mo, 23 mo, 8 yr, 14 yr, 21 yr; clearance and retained dose also simulated
Ultman	Factors influencing the dosimetry of reactive gases in children	Diffusion-reaction model of reactive gas deposition including a mucus layer run for ozone at ages 0, 4, 8, 12, and 16 yr under varying activity levels
Kimbell	Nasal imaging and computational fluid dynamics-based dosimetry models	CFD modeling techniques as applied to children
Jarabek	The challenge to children's dosimetry modeling: creating a context for comparative analysis and consistent application in risk assessment	1994 RfC hierarchical framework for model structure evaluation; decision analytical framework for comparison of model structure, output, reliability and relevance to mode of action, variability and uncertainties

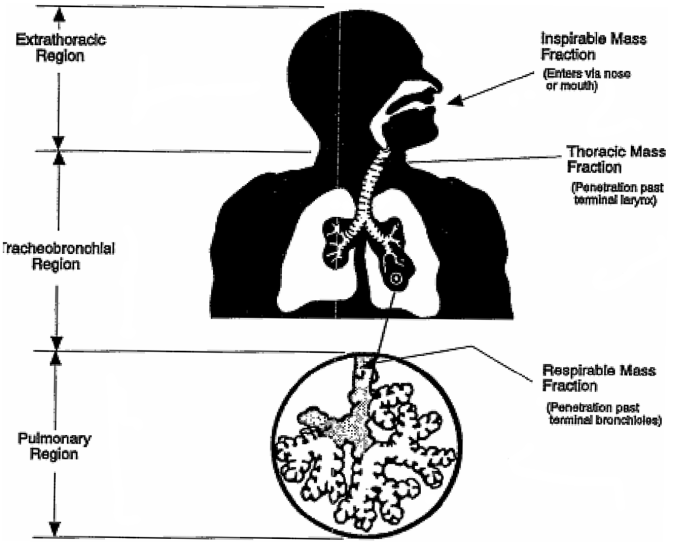

FIG. 1. Diagrammatic representation of three respiratory-tract regions. From U.S. EPA (1994).

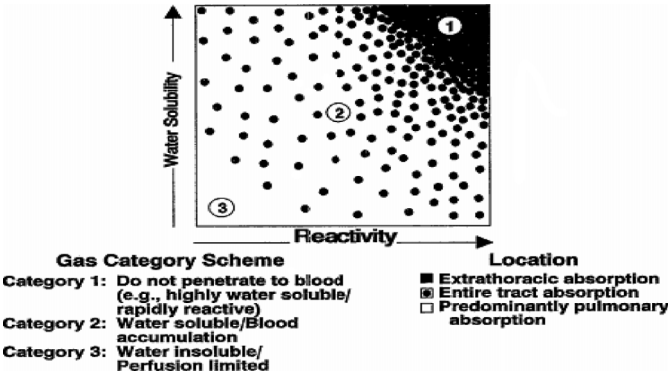

FIG. 2. Gas categorization scheme based on water solubility and reactivity as major determinants of gas uptake. From U.S. EPA (1994).

scheme for different types of gases that would help motivate different modeling approaches to describe dosimetry and arrive at dose estimates for each (U.S. EPA, 1994). The gas category scheme provides a framework for choosing an appropriate model structure that captures critical physicochemical properties of the inhaled gas and its interaction with physiological characteristics of the various respiratory tract regions. The goal is a description of the dosimetry of inhaled gases that is commensurate with the available data and level of detail regarding the mode of action for toxicity (Jarabek, 1995a). Although it should be recognized that the gas category scheme represents a continuum and that the same broad model structure may be applied to all categories, a review of the principles and properties informing category-specific default algorithms is helpful to understanding the dominant determinants of gas uptake in each region (Hanna et al., 2001). The framework motivated many of the modeling efforts described herein for reactive gases in the upper respiratory tract (URT) (Andersen and Jarabek, 2001).

Category 1 gases (e.g., chlorine, formaldehyde, vinyl acetate) are either water soluble or reactive[1], and are thus scrubbed out of the inhaled air primarily in the ET region at low exposure concentrations. Such gases typically exhibit a proximal to distal penetration and toxicity profile with increasing exposure concentration (U.S. EPA, 1994; Jarabek, 1995a). High levels of deposition in discrete regions of the nose combined with high reactivity leads to the potential for localized tissue damage (Morgan, 1994; Kimbell, et al., 1997). Only a small percentage of a Category 1 gas penetrates beyond the ET at low concentrations typical of ambient exposures, with this penetration greatest during exercise when ventilation rates are the highest (U.S. EPA, 1994; Nodelman and Ultman, 1999).

Category 2 gases are intermediate in reactivity and water solubility, which allows them to penetrate more readily beyond the ET and into the bronchi, and to a lesser extent the PU region. Some have the potential to accumulate in blood and thus have systemic as well as local effects, or may also deliver the toxicant back to the airway tissues from the endothelial side (U.S. EPA, 1994; Jarabek, 1995a). While not as reactive as Category 1 gases, Category 2 gases such as ozone (O_3) still attack cellular constituents. Their potential to produce damage may be enhanced because they penetrate deeper into the airways where the protective mucus layer is thinner (Chang, et al. 1992; U.S. EPA, 1994). However, mucus is not always effective as a protective barrier since toxic reaction products can form in mucus and these penetrate to underlying epithelial tissue (Ferng, et al. 1997). Category 3 gases, such as the chlorinated solvents chloroform and trichloroethylene, are non-reactive in the respiratory epithelium and not water soluble. They are not scrubbed out in the conducting airways but instead penetrate to the PU region where they are absorbed into the systemic circulation. Their toxicity is typically related to metabolic activation in liver and kidneys, or delivery of parent compound to the CNS.

This outline of particle and gas deposition points to the importance of the ET region in removing larger particles and reactive gases from the inhaled airstream. Air traversing the oral passages encounters less surface area than air that is inspired nasally, and toxicant removal in the nasal passages is more efficient due to smaller airway dimensions (Heyder, et al. 1975). Therefore, the dose that is available to the deeper airways is generally larger from oral as opposed to nasal breathing. Nasal breathing predominates at low to moderate ventilation rates but is augmented with oral breathing at higher rates that are associated with exercise and exertion (Niinimaa

[1] The U.S. EPA included in its definition of reactivity the ability of the inhaled gas to serve as a substrate for metabolism in respiratory tract tissues. For example, vinyl acetate, while not especially water soluble, is readily extracted in the URT via carboxylesterase metabolism and is considered a Category 1 gas.

et al., 1981; ICRP, 1994; Bennett et al.,2008).Given that children's activity and ventilation patterns are different than those of adults, it is possible that the oral-to-nasal ratio may be another age-specific factor that affects inhalation dosimetry.

The manner in which the various factors described above (particle size, reactivity of gases, ventilation rate, respiratory surface area, and oral-to-nasal ratio) affect inhalation dosimetry in children and adults are explored through various modeling techniques in subsequent sections.

APPLICATION OF DEFAULT INHALATION DOSIMETRY MODELS TO EVALUATE CHILD-ADULT DIFFERENCES IN REGIONAL AND SYSTEMIC DOSE

Risk assessment of inhaled toxicants often involves cross-species extrapolation of an inhaled dose associated with an effect observed in a laboratory test species. Models used for this extrapolation range from rudimentary forms with a minimal number of parameters that accommodate sparse databases, to more sophisticated structures with detailed mechanistic descriptions of tissue responses (Jarabek, 1995b). The U.S. EPA (1994) provided a hierarchical and flexible framework for evaluating when alternate structures offered advantages to the default algorithms. Characteristics of models that would be considered "preferred or optimal" relative to "default" structures are shown in Table 2 (U.S. EPA, 1994). Considerations include whether the model utilizes chemical- and species-specific mechanistic information or rather relies on categorical, empirical parameters for key determinants such as ventilation and metabolic rates. For the default descriptions, the U.S. EPA's 1994 reference concentration (RfC) methods introduced rudimentary models that relied on predominantly empirical descriptions of particle deposition and gas uptake, but nonetheless also represented reduced forms consistent with more sophisticated, detailed structures. For example, the gas-phase mass transfer coefficient used in the RfC methods is analogous to those used for models of O_3 and formaldehyde (Hanna et al., 2001; Kimbell et al., 2001a; Overton and Graham, 1989), and the inhalability adjustments and fractional deposition algorithms are analogous to those used in the ICRP and multiple-path particle dosimetry (MMPD) particle models described below. What distinguishes these models is the degree of detail and data underlying different descriptions (e.g., delineation of bronchioles and interstitial compartments in the ICRP model, localized gas flux estimates within the URT for formaldehyde uptake in the CFD models).

TABLE 2
Hierarchy of Model Structures for Exposure-Dose-Response and Interspecies Extrapolation

"Optimal" model structure
• Structure describes all significant mechanistic determinants of chemical disposition, toxicant–target interaction, and tissue response
• Uses chemical-specific and species-specific parameters
• Dose metric(s) described at level of detail commensurate to toxicity data
Default model structure
• Limited or default description of mechanistic determinants of chemical disposition, toxicant-target interaction, and tissue response
• Uses categorical or default values for chemical and species parameters
• Dose metric(s) at generic level of detail

Note. Source: U.S. EPA (1994).

While this framework was useful in developing risk estimates for interspecies extrapolation from lab animal inhalation toxicology studies, the RfC methodology did not explicitly include adjustments to account for the physiological and anatomical differences that occur throughout a lifetime. Potential uncertainty in resultant risk estimates due to variability across life stages was believed to be addressed by the various uncertainty factors (UF) applied in operational derivation of the RfC including those specifically recognized for intrahuman variability and database deficiencies. However, recent emphasis on children's risk (Landrigan, 1999; FQPA, 1996) warrants exploration of modifying available dosimetry models to account for children's dosimetry directly, as well as for evaluating the adequacy of the methodology as a whole, including the intrahuman and database UF, in light of such simulations.

At about the same time, the International Commission on Radiological Protection (ICRP, 1994) developed a respiratory tract dosimetry model for the assessment of exposure from inhaled radionuclides. The ICRP approach is more inclusive than the RfC methodology by utilizing activity patterns for a wide range of children's age groups beginning with 3 months of age as input to the model. Further, as a semi-empirical model that includes some theoretical and mechanistic algorithms, the ICRP model includes explicit descriptions of various particle deposition mechanisms, e.g., particle impaction (based upon particle size and air velocity) and deposition via diffusion (based upon diffusion coefficient in air). Because the RfC methods rely on an empirical model description of deposition data that did not include particles of the diameter subject to diffusion as a dominant mechanism of deposition, the RfC model is not recommended for extrapolation outside that range (Raabe et al, 1988; U.S. EPA, 1994). As such, the ICRP model may provide a more reasonable model for the broader range of particle sizes with which to extrapolate to different ages based on varying ventilation rates, and may provide better estimates of regional inhaled dose than the regional empirical descriptions in the RfC methods. For example, the ICRP model divides the TB region into the more proximal portion (to generation 8) and the bronchioles (below generation 8).

Inclusion of activity patterns and age-specific ventilation rates to calculate children's risk using the ICRP model was a critical component of the Agency's effort to update the National Ambient Air Quality Standards (NAAQS) for particulate matter (PM) in 1996, and similar simulation exercises with these activity patterns were performed with the MPPD model for the Agency's 2005 assessment and standard setting. Thus, exploration of using age-specific ventilation rates in other risk assessment arenas may benefit from a similar approach.

GENERAL MODELING APPROACH

The default modeling approaches used to compare a 3-month old infant and adult respiratory tract dosimetry are depicted in Figure 3.

Particle deposition simulations using the default models and in the more refined modeling approaches described later in this paper estimate dose as the amount of toxicant delivered to a particular region per unit time normalized to surface area. The rate of clearance from that region to estimate retained dose was not considered. Thus, delivered rather than retained dose is described.

Since both the default RfC models and ICRP models were used to assess particle deposition, comparisons were made not only across age groups but also across default models. For particles, deposition was either calculated from the equations in the RfC methodology or was taken directly from the deposition fractions provided by the ICRP model and then normalized to surface area to calculate the dose metric compared between the models. Runs of the RfC model are truncated for particle sizes below 1 μm. These particles are subject to diffusion and are below the range in which this model was calibrated. The incorporation of children's parameters into these models represents scaling of the adult architecture and does not necessarily reflect an accurate comparison of airway structure or morphometry across life stages. For example, the ICRP model structure was adapted to that of a 3-month old infant by scaling and calculations based upon airway cast measurements as shown in Table 3. It was also run with adult parameters to compare estimates of delivered dose between children and adults. Three months of age was chosen as the mid-point for the first 6 months of life, a time when child-adult differences in ventilation rate per lung surface areas are likely to be greatest. The adult male parameters of the ICRP were used to calculate the adult estimates presented (ICRP, 1994).

Both the particle and gas uptake models were run under nasal breathing, light activity conditions to represent the most common breathing pattern, although it is recognized that

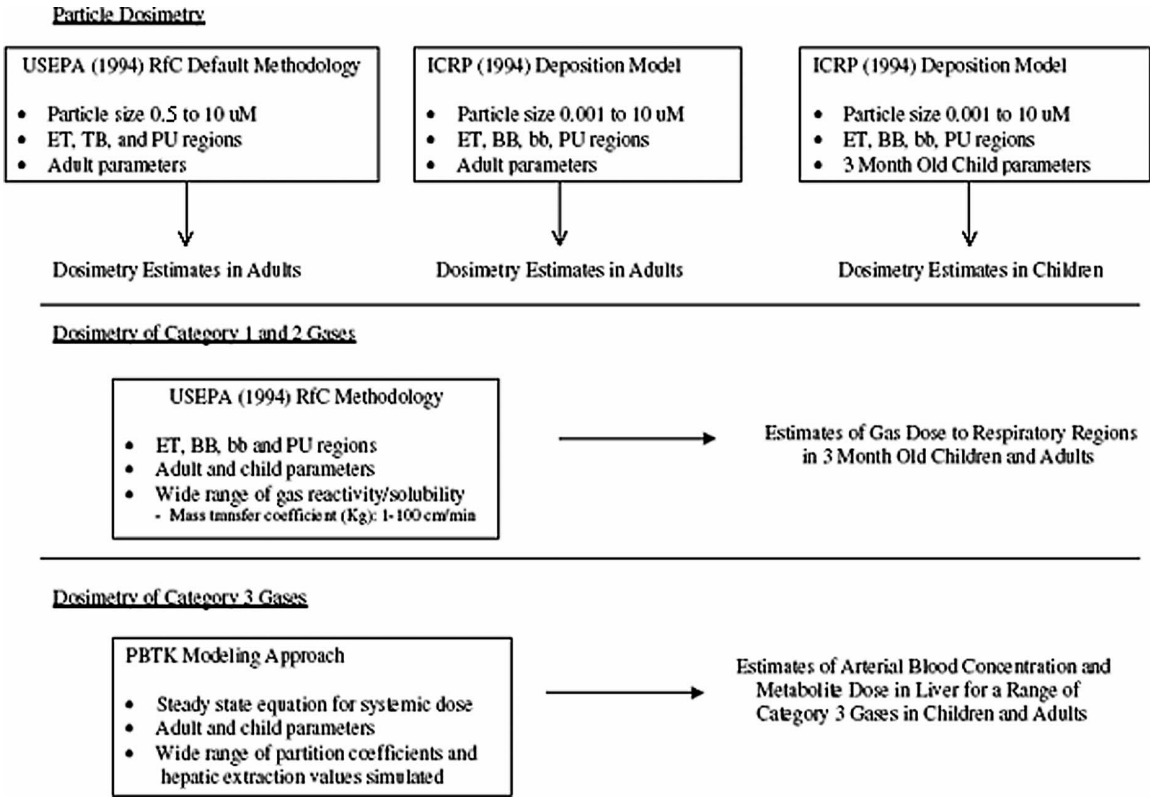

FIG. 3. Approach for dosimetry comparisons across default models in 3-mo-old infant and male adult. Modified from Ginsberg et al. (2005).

TABLE 3
Regional Surface Areas (cm^2) and Ventilation Rates in 3-mo-Old Infant and Adult Male

	Current analysis			RfC methodology[a]
Region	3 mo	Adult male	Data source	Adult male
ET[b]	40	160	Sarangapani et al. (2003) based upon age-related changes in cranial size from CT scans	200
TB[c] upper(BB)[d]	58	283	Phalen et al. (1985) scaling parameters and surface area calculations based upon surface area of a cylinder	3200[e]
TB lower(bb)[f]	1512	2080	Phalen et al. (1985) scaling parameters as for TB region	—[e]
PU[g]	37704	777417	Yu and Xu, 1987 equations for alveoli number and dimension increase with age	540,000
Ventilation rate (ml/min)	2372	13800	Rate for light degree of activity (Harvey and Hamby, 2002; Sarangapani, et al., 2003)	13,800

Note. Adapted from Ginsberg et al. (2005).
[a] U.S. EPA (1994).
[b] ET = extrathoracic region of respiratory tract.
[c]TB = tracheobronchial region of respiratory tract.
[d]BB = bronchi generations 1–8 as per ICRP (1994).
[e]RfC methodology does not treat bronchi and bronchiolar regions as separate, so that the surface area shown for TB is the sum of both upper and lower bronchial regions.
[f]bb = Brionchioles: generations 9 and below as per ICRP (1994).
[g]PU = pulmonary region of the respiratory tract.

higher ventilation rates and switchover to oral breathing might lead to deeper penetration of particles and gases in both children and adults (U.S. EPA, 1994). A wide variety of particle sizes and gas reactivities were modeled in this screening exercise to evaluate whether certain combinations of toxicant properties and respiratory regions might lead to substantial child-adult dosimetry differences.

Reactive gas modeling for children (3-month old infant) and male adults was simulated for gases with a variety of reactivities by using a range for the overall mass transfer coefficient (K_g) from 1 to 100 cm/min. This parameter is typically measured empirically in isolated regions of the respiratory tract and takes into account the net transfer of the gas due to convection and molecular diffusion in the air-phase, water solubility and chemical reactivity (e.g., hydrolysis), diffusion, and metabolism in the liquid lining and tissue phases, as well as clearance into the blood (Hanna et al., 2001; Andersen and Sarangapani, 2001). The Kg is thus an empiric measure of total flux from the air into the mucus or tissue layer and is both a species- and an age-specific parameter. This is related to the fact that convection (bulk flow due to ventilation) and diffusion thicknesses that govern Kg are dictated by airway architecture for the lumen and tissue.

The Kg is used to predict the amount of toxicant that actually interacts with cellular constituents and is often the key input parameter to physiologically-based pharmacokinetic (PBPK) models that provide more detailed mechanistic descriptions of reactions within different tissue types as described in Section 5 below. Category 1 gases such as chlorine, formaldehyde, hydrogen fluoride, and organic acids and esters have K_g values in the upper end of this range and are scrubbed out of the airstream primarily in the ET region (Nodelman and Ultman, 1999; Overton, 2001; USEPA, 1994). Category 2 gases such as O_3 and sulfur dioxide (SO_2) are represented in this modeling framework by a K_g value of 20 cm/sec, which leads to 20–30% uptake in the upper airways and the majority of the dose deposited in the lower conducting airways (bb region). This is consistent with modeling estimates of O_3 uptake in humans and animal inhalation experiments showing that the majority of O_3 uptake is in more distal regions of the respiratory tract (Miller et al., 1985; Overton, et al., 1987; Grotberg, et al., 1990; Sarangapani, et al., 2003; ICRP, 1994).

For non-reactive gases, the steady-state approach described in the RfC methodology was enhanced by the explicit inclusion of parameters representing hepatic blood flow and intrinsic clearance (Sarangapani, et al., 2003; RfC Methodology, Appendix I) to describe blood levels of parent compound and hepatic levels of metabolite. The steady state model was run with parameters for male adults and 3-month old infants, with

additional runs conducted for 1-year olds. Details of the methods and equations used for these simulations are described elsewhere (Ginsberg, et al., 2005).

The key physiological parameter governing deposition of particles and gases in the RfC and ICRP default models is ventilation rate. If the chosen dose metric is the deposited fraction normalized to surface area, as proposed in the RfC methods, then regional surface area is also an important normalizing parameter in the calculation. The characteristics of the inhaled material, in particular particle diameter and its distribution, are key determinants of deposition as well. Parameter values for 3 month old children and adults are presented in Table 3. The largest difference in ventilation rate per surface area across age groups is in the PU region as neonates have relatively few alveoli at birth, leading to a large ratio of air flow per surface area in the 3 month old deep lung. The opposite situation exists in the bronchioles (bb region) in that its branched airway structure is believed to be nearly complete at birth leading to a relatively large surface area even at young ages.

DEFAULT MODEL RESULTS FOR YOUNG CHILDREN

Particle deposition modeling results for the major respiratory regions are presented as average dose normalized to regional surface area (μg deposited/cm^2/min) in Figures 4 to 7. Deposition estimates for the ET region show agreement between the RfC and ICRP models in the larger particle size range (> 1 μm); however, comparisons across models are not possible below that range. Comparison of predictions for the 3-month old infant to male adult using the ICRP model did not reveal substantial differences in deposition in the ET region. Figure 5 shows a generally similar pattern predicted in the upper TB region with results for the 2 models and for the 2 age groups converging in the 1–10 μm size range. Ultra fine particles having a diameter below 0.1 μm are predicted to have nearly 2-fold higher dose in a 3-month old infant than in male adults. This profile reverses in the bronchiolar region as adult dosimetry is greater than in the 3-month old for ultra-fine particles (Figure 6). This prediction may be in part due to the scrubbing out of ultra-fine particles in more proximal airways, which appears to be greater in children, and in part to the high surface area already developed in 3-month old bronchioles. Deposition predictions for the PU region shows greater deposition in a 3 month old infant compared to male adults for ultra-fine particles (Figure 7). The differential is approximately 2–4 fold. As with the other regions, model output for the 1–10 μm range shows little across age or across model difference. Thus, if one were modeling particles in this size class only, the default RfC algorithm would yield results for adults that would also be reasonable estimates for young children. However, to address smaller particles, other models such as the ICRP or MPPD models would need to be used.

Results from using the default gas dosimetry algorithm across the spectrum of K_g values and for various regions of the respiratory tract are shown in Figure 8. It should be noted that for these calculations, the parameter value for K_g was assumed to be the same along the entire respiratory tract, and also to be the same in adults and children, despite differences that would occur due to differences in architecture noted above if the Kg were actually measured. As anticipated for Categories 1 and 2

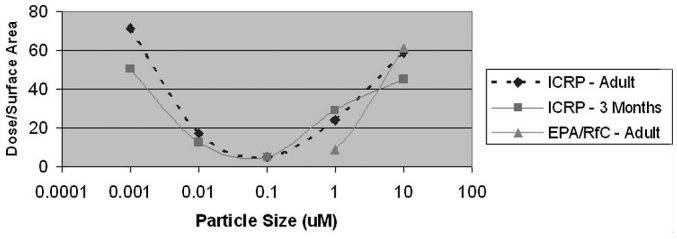

FIG. 4. Particle deposition predicted by various models in the ET region of 3-mo-old infants and male adults. Dose per surface area units in μg/cm^2/min at an inspired concentration of 1 μg/ml. Simulations used ICRP (1994) or U.S. EPA RfC methodology (1994) models. Adapted from Ginsberg et al. (2005).

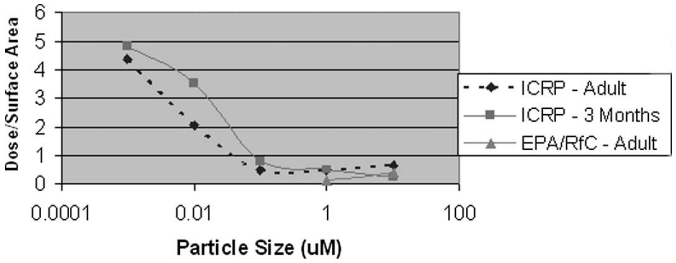

FIG. 5. Particle deposition predicted by various models in the upper trachea/bronchii (bb) region of 3-mo-old infants and male adult. Dose per surface area units in μg/cm^2/min at an inspired concentration of 1 μg/ml. Simulations used ICRP (1994) or U.S. EPA RfC methodology (1994) models. Adapted from Ginsberg et al. (2005).

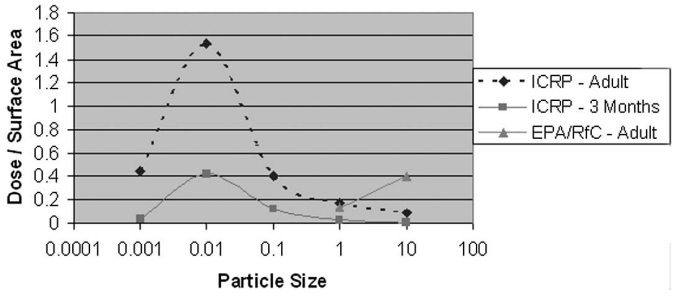

FIG. 6. Particle deposition predicted by various models in the bb (bronchiolar) region of 3-mo-old infants and male adults. Dose per surface area units in μg/cm^2/min at an inspired concentration of 1 μg/ml; particle size in micrometers. Simulations used ICRP (1994) or U.S. EPA RfC methodology (1994) models. Adapted from Ginsberg et al. (2005).

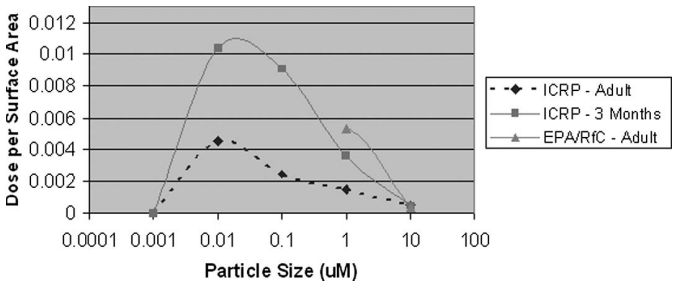

FIG. 7. Particle mass deposition predicted by various models in the PU region of 3-mo-old infants and male adults. Dose per surface area units in μg/cm^2/min at an inspired concentration of 1 μg/ml. Simulations used ICRP (1994) or U.S. EPA RfC methodology (1994) models. Adapted from Ginsberg et al. (2005).

gases, these calculations predict extraction of high K_g gases occurring mainly in the ET region, with greater penetration of gases of intermediate reactivity (Category 2). As K_g decreases further to the low end of the range simulated, a substantial portion reaches the PU region. At this low reactivity it is likely that much of the deposited dose would be systemically absorbed rather than react locally. The modeling of the systemic absorption of gases with low reactivity (Category 3) is described below.

For interspecies extrapolation of respiratory tract effects, gas uptake is typically normalized to surface area to calculate the default regional gas dose (RGD) used in a ratio (relative to the human RGD) as the interspecies dosimetric adjustment factor (DAF) in the RfC methods. Figure 9 shows estimates of the RGD for 3 month old children and adults, across the same range of K_g values as shown in Figure 3–6, expressed as mg/cm^2-min for a 1 mg/ml inspired concentration. Overall, the simulations show estimated RGD values that are greatest in the ET region where there is the highest rate of gas delivery per surface area. This is especially pronounced for high reactivity/solubility gases for which there is little penetration beyond the initial airway regions. The RGD generally declines with increasing distance in the respiratory tract due to less gas delivery to these regions. The estimated RGD values for 3 month old children are not markedly different from adult values. The increased % gas extraction in the bb region of 3 month old children (Figure 8) is counterbalanced by the lower rate of gas delivery to this region in this age group. This leads to RGD values that are somewhat lower than adult levels. At the lowest reactivity assessed (K_g=1 cm/min) the dose to the PU region becomes greater in 3-month old infants than male adults but the reverse is true for K_g=5 cm/min, and in any case, RGD values in the PU region are still far below those in more proximal regions. These default modeling calculations suggest only minor differences in predicted respiratory dosimetry of reactive gases when comparing between 3-month old infants and male adults, but may largely reflect the assumption that the Kg was the same across the age groups.

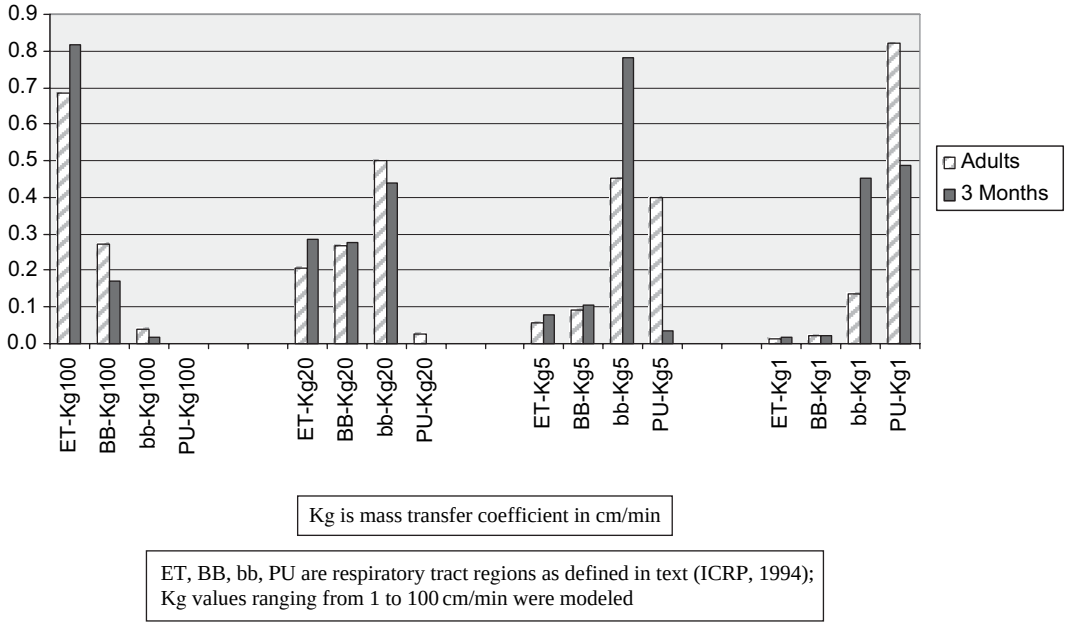

FIG. 8. Percent extraction of reactive gases predicted by RfC methodology (U.S. EPA, 1994) in the respiratory tract of 3-mo-old infants and male adults. From Ginsberg et al. (2005).

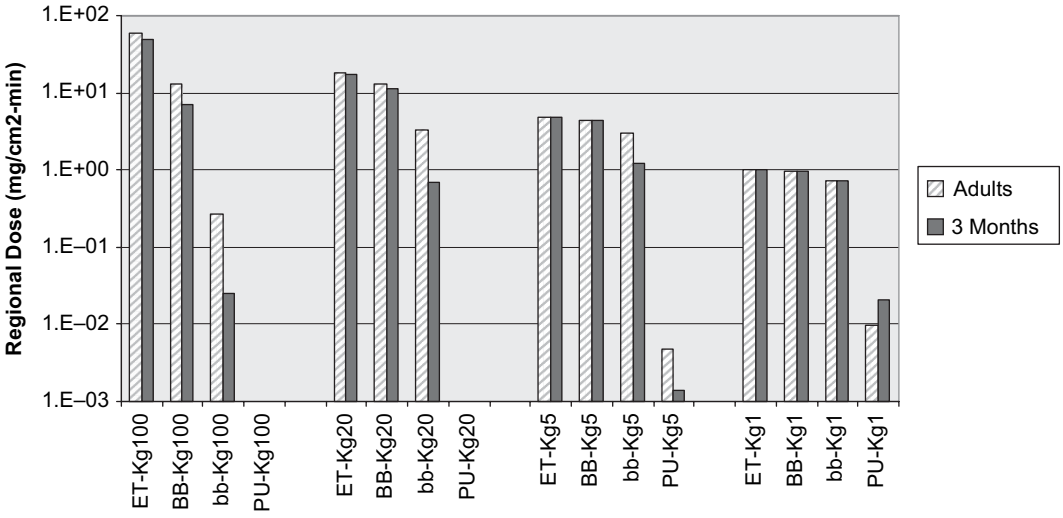

FIG. 9. Reactive gas dosimetry predicted for respiratory regions of 3-mo-old infants and male adults by the default model. ET, BB, bb, PU are respiratory tract regions as defined in text (ICRP, 1994); K_g is mass transfer coefficient in cm/min. K_g values ranging from 1 to 100 cm/min were modeled. From Ginsberg et al. (2005).

Rather than simulating specific Category 3 gases, Ginsberg et al. (2005) constructed a matrix of gases having a range of blood: air partition coefficients and intrinsic hepatic clearance. All gases were assumed to be substrates for CYP2E1, the hepatic CYP most commonly involved in metabolizing chlorinated solvents and simple aliphatic molecules (Guengerich, et al., 1991). Therefore, the developmental profile for this CYP was used to adjust intrinsic clearance for children at 3 months (30% adult function, Vieira, et al. 1996; Alcorn and McNamara, 2002). Figure 10 shows that gases which are readily extracted by the liver yield nearly a 2 fold more liver metabolite dose in 3-month old infant than adults. This is related to the fact that at such high extraction rates, hepatic blood flow is the rate limiting step to metabolic clearance, with this limitation preventing the expression of the metabolic immaturity in CYP2E1 at this age. In contrast, parent compound blood concentrations are greater in children than in adults for low extraction chemicals since this is where the immaturity in CYP2E1 makes the biggest dosimetry difference. This pattern is accentuated in other simulations involving clearance by a CYP that is slower to mature (e.g., CYP1A2; Sonnier and Cresteil, 1998) (data not shown).

The ventilation rates for young children selected in these model exercises are low relative to those estimated by an alternative method for deriving inhalation rates recently published and presented at this workshop (Foos, et al., 2007; U.S. EPA,

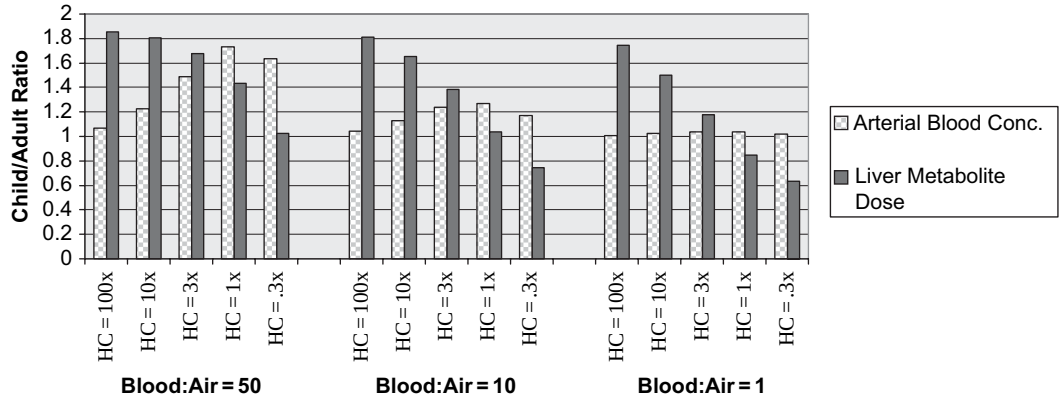

FIG. 10. Comparison of infant–adult internal dosimetry predicted for a range of Category 3 gases using the steady-state default model as described in U.S. EPA (1994) and Sarangapani et al. (2003). HC signifies hepatic clearance relative to blood flow; blood:air partition coefficients ranging from 1 to 50 were modeled. From Ginsberg et al. (2005).

2006). The newer estimates are based upon basal metabolic rate and energy expenditure at different levels of activity represented in the Comprehensive Human Exposure Database (CHAD) described in a companion paper (Foos, et al., 2007). These inputs are then used to calculate oxygen (O_2) demand and the ventilation rate needed to support this O_2 demand. Use of these updated estimates would generally lead to greater child-adult differences in deposition in the exercises performed herein because of the sensitivity of the model to the ventilation rate input parameter.

CONCLUSIONS FROM USE OF DEFAULT MODELS

Default models and algorithms were used in the assessment of risk from inhaled chemical and PM exposures for more than a decade. While they represent simplistic descriptions of gas uptake and particle deposition based largely on empirical measurements, they provide a useful default or screening level analysis of cross-chemical and cross-species differences in respiratory dosimetry. As shown above, they also were adapted to provide comparisons across age groups and thus inform risk assessments of inhaled toxicants in children. The simulations and calculations in this section suggest that 3-month old infants may receive a greater delivered dose of inhaled PM, especially for ultra-fine particles in the PU region. While reactive gas dosimetry did not show marked child-adult differences, this might change if the estimates of child ventilation rates derived from the alternative method discussed above are validated for use in dosimetry modeling. Internal dosimetry of Category 3 gases may be greater in children than adults with the difference (1) depending upon the chemical's blood:air partition coefficient, (2) rate of hepatic metabolism, and (3) whether the parent compound or metabolite is of most concern. Estimates of children's dosimetry may be improved with the development of more refined modeling as described in subsequent sections of this paper, and these improvements need to be incorporated into generally applicable models that are suitable for risk assessment.

MULTI-PATHWAY MODELING OF PARTICLE DOSIMETRY IN THE RESPIRATORY TRACT OF CHILDREN

Chronic exposure to airborne PM is associated with increased morbidity and mortality, particularly in sensitive populations such as the elderly and children (Berglund et al., 1999; Beyer et al., 1998; Conceição et al., 2001; Gauderman et al., 2002). Most efforts to characterize the fate of inhaled particles in the lung have focused on adults, and few studies are available in children. Children present a special challenge because the growth and development of the airways are not fully characterized especially with respect to the degree that these vary at a particular age. Given that lung physiology and geometry differ markedly between children and adults (Overton and Graham, 1989), it is important to explore dosimetry models that predict the deposition and clearance of PM in the extrathoracic and lower respiratory tract (LRT) airways of children.

EXTRATHORACIC (ET) PARTICLE DEPOSITION: MEASUREMENTS AND MODELING IN CHILDREN

Morphometric studies of the ET airways were documented from cadaver studies in children (Bosma, 1986). However, the anatomical dimensions produced from this work are believed to overestimate nasal airway dimensions *in vivo* due to decongestion, dehydration, and fixation artifacts (Swift, 1991). Previous studies in adults using magnetic resonance imaging (MRI) showed that the average cross-sectional area of airways *in vivo* was 33–50% (Guilmette et al., 1989) of that described in cadaver studies (Montgomery et al., 1979). These differences make MRI or CT data preferable when available for children and adults such as reported in hollow airway models (Swift 1991; Swift et al. 1994; Janssens et al. 2001). In these projects, a 4-week old infant (Swift et al., 1994), a 6-week-old infant (Swift, 1991) and a 9-month-old child (Janssens et al., 2001) were included. Particle deposition studies in these hollow airway models were conducted for a variety of particle sizes using spherical aerosol particles. However, the model of Janssens et al. (2001) is the only one that includes a larynx, which is a key anatomical feature for deposition of inhaled PM.

A number of models are used to predict particle deposition in the ET airways of young children and adolescents. Xu and Yu (1986) and Robinson and Yu (2001) simply use adult ET airway values and do not scale for children and adolescents. The ICRP (1994) models scale the ET airways as a function of tracheal diameter, as suggested by Yu and Xu (1987). The NCRP (1997) model uses an empirical equation derived from adult clinical data and assumes that children and adults possess the identical deposition efficiency at equivalent physical exertion levels. Recently, Cheng (2003) proposed empirical equations for particle losses due to diffusion and impaction in nasal and oral airways. These equations are based on clinical measurements in adults and *in vitro* measurements in hollow nasal and oral models.

Direct use or rescaling of the adult models based on tracheal diameter may lead to deposition overprediction and underprediction in the ET and lung respectively, in children (Asgharian, et al., 2004). While limited, it is best to use existing measurements to construct semi-empirical models of particle deposition in the ET region of children. For example, deposition measurements of 1– to 2– um particles in the nasal airways of children in two age groups above and below 11 years are reported by Becquemin et al. (1991). Asgharian et al. (2004) developed models of ET deposition by impaction by fitting the above dataset to a functional relationship between particle deposition efficiency and impaction parameter. Similar

relationships are desirable for nano-sized and ultrafine particles in nasal airways and for all size particles in oral airways. At this time these remain important data gaps.

LOWER RESPIRATORY TRACT GEOMETRY: MEASUREMENTS AND MODELS IN CHILDREN

Information on the lung geometry of children for use in particle deposition models is also extremely limited. A child's lung is not a scaled-down version of an adult lung, so that direct measurements are requisite for accurate descriptions of particle deposition in various age groups. It is generally agreed that the number of bronchial airways are complete at birth (Reid, 1984), but the rate of growth of proximal and distal airways changes with age. The alveolar region consists of respiratory bronchioles, ducts, and a terminal cluster of alveolar sacs at birth (Charnock and Doershuk, 1973). The number and size of alveoli increase with age, with the number stabilizing before the age of 8 (Dunnill, 1962; Reid, 1984).

Despite these data limitations, several models of bronchial airway growth in children were proposed (Xu and Yu, 1986) using some simplified scaling approaches. These models assume the same growth rate for all airways, the same as those of main bronchi. Phalen et al. (1985) proposed a different model of airway growth from measurements of the right upper lobe of 20 casts of children's lungs. They found a relationship between airway size and subject body length per airway generation. The children's geometries used in the ICRP (1994) and NCRP (1997) dosimetry models are based on the data of Phalen et al. (1985). Thus, these geometry models may not be true representations of lung geometry in the sense that they are based on a limited dataset.

Additional information on children's lung airway parameters is available. Mortensen et al. (1983) at the Utah Biomedical Test Laboratory (UBTL) made complete measurements of tracheobronchial (TB) airway lengths, diameters, and branch angles for the first 10 generations of the lungs of 11 children between 3 months and 21 years old. Ménache et al. (personal communication) developed single-path, whole-lung and lobar lung models for children based on this dataset and information on distal airway dimensions published in the peer-reviewed literature (Weibel, 1963). First, the number of conducting airway generations was estimated from available information in the literature (Weibel, 1963; Yeh and Schum, 1980; Horsfield and Cumming, 1968; Beech et al., 2000). An average of 16 generations was used for the conducting airways in the typical-path model. This number for the lobar model consisted of 15 generations in the right upper, right middle, and left upper lobes, and 16 and 17 generations in the left and right lower lobes respectively. In addition, three generations of respiratory bronchioles and 4 generations of alveolar ducts were selected (Pinkerton et al., 2000; Weibel, 1963; Yeh and Schum, 1980; Horsfield and Cumming, 1968; Haefeli-Bleuer and Weibel, 1988; Hislop and Reid, 1974; Reid, 1984).

Ménache et al. (personal communication; Asgharian, et al., 2004) then determined airway dimensions for the conducting and respiratory airways. Measurements from Mortensen et al. (1983) were used for the first 10 generations of the lobar models. The airway dimensions of the typical model in the first 10 generations were simply averaged length and diameter values per generation. For the remaining airway generations, Ménache et al. (personal communication) used an equation proposed by Weibel (1963) to estimate the missing dimensions in each generation. The equation proposed by Weibel (1963) related airway dimensions (e.g., length and diameter) to generation number. The coefficients of the equation were obtained by fitting the equation to the airway dimensions of the first 10 generations plus published airway dimensions of the terminal bronchioles, respiratory bronchioles, alveolar ducts, and alveolar sacs.

Finally, Ménache et al. (personal communication; Ashgarian, et al., 2004) used available information to estimate the following for the respiratory airways at different age groups: number (Weibel, 1963; Dunnill, 1982; Thurlbeck, 1988), diameter (Hislop et al., 1986; Dunnill, 1962; Weibel, 1963), and distribution of alveolar volume (Weibel, 1963; Haefeli-Bleuer and Weibel, 1988). This resulted in typical-path and 5-lobe symmetric but structurally different lung geometries for 11 age groups ranging from 3 months to 21 years. The completed airway model was uniformly scaled to predicted functional residual capacity. The expressions derived by Overton and Graham (1989) were used to estimate lung and breathing parameters at each age group.

LOWER RESPIRATORY TRACT: PARTICLE DEPOSITION MODELING IN CHILDREN

A variety of mathematical models were developed to predict particle deposition in the respiratory tract. The range of models extends from empirical models that do not incorporate lung geometry explicitly (Rudolf et al., 1986, 1990; ICRP, 1994), to typical-path models (Yu, 1978) based on symmetric lung geometry, and mathematically more complex, multiple-path models that are based on asymmetric lung structure (Anjilvel and Asgharian, 1995; Asgharian and Anjilvel, 1998; Asgharian et al., 2001). In addition, there are stochastic lung deposition models that sequentially generate one airway at a time along a given lung pathway and calculate particle deposition for that airway. By repeating deposition calculations along many randomly-generated pathways, an average deposition fraction is calculated statistically (Koblinger and Hofmann, 1985, 1990). While empirical models are accurate and easy to use, they can not be used to extrapolate outside the range of measured data (e.g., the range of particles sizes used to measure deposition efficiency). Typical-path lung models are useful for obtaining average regional and overall deposition of particles in the lung but do not provide information regarding distribution of deposited particles in the lung. More detailed

and site-specific deposition information are gained by using deterministic and stochastic multiple-path deposition models in which more accurate assessment of the lung structure is included.

The multiple-path particle dosimetry (MPPD) model calculates deposition fractions of inhaled particles in all airways of the respiratory tract during a single breathing cycle (CIIT Centers for Health Research, 2004). In general, the process of deposition modeling in the MPPD model consists of 4 steps. First, lung ventilation is calculated to determine how the inhaled particles are distributed throughout the lung. For a uniformly expanding and contracting compliant lung, airflow rate at any location in the lung is proportional to the volume distal to that location. Second, the combined deposition efficiency of particles in each airway by various deposition mechanisms is calculated. Deposition efficiency is the fraction of traveling particles through an airway that are deposited as a result of external forces exerted on them. Third, particle transport in the lung is simulated by solving the transport equation shown below to yield particle penetration and deposition. The transport equation in a uniformly expanding and contracting lung is described by the following expression:

$$\frac{\partial}{\partial t}(Ac)+\frac{\partial}{\partial x}(Qc)=-\lambda c \tag{1}$$

where A is the airway cross-sectional area, c is particle concentration, Q is the airflow rate, γ is related to particle deposition efficiency, and x and t are distance along the airway and elapsed time respectively. Equation (1) is solved by method of characteristic to find particle concentration at the exit of the airway.

The last step in deposition modeling involves performing a mass balance on the particles in the lung to calculate fraction of inhaled particles that are deposited per airway, generation, region, and lobe of the lung. Assuming a steady-state, steady-flow process, the mass balance on the traveling particles in an airway during a single breathing cycle (inhalation, pause, and exhalation) written in the following form:

$$m_{dep} = m_{ini} + m_{in} - m_{out} - m_{rem} \tag{2}$$

where m_{dep} is the mass deposited in an airway, m_{ini} is the mass initially in the airway, m_{in} and m_{out} are the masses of particles that enter and leave the airway at the end of the breath, respectively, and m_{rem} is the undeposited mass in the airway.

The MPPD model for deposition in children is practically identical to the MPPD model for adults except for the differences in lung geometry and lung and breathing parameters, which may be due to assumptions regarding scaling. Earlier deposition models for children are based on simplified typical-path lung structures that were obtained from limited airway measurements in children's lungs (Phalen et al., 1985) and are useful for regional prediction of deposition. The availability of lobar lung geometry (Ménache et al., personal communication) paved the way for more advanced deposition modeling in the lungs of children. Asgharian et al. (2004) used the lung geometries from Ménache et al. (personal communication) and developed a lobar deposition model for children based on the multiple-path analogy described above. The MPPD model is used below to compare deposition between children and adults (Asgharian et al., 2004; CIIT Centers for Health Research, 2004).

RESULTS OF THE MULTIPLE-PATHWAY PARTICLE DOSIMETRY (MPPD) MODEL IN CHILDREN

Measurements of particle deposition fraction in the thoracic airways of children via oral breathing was reported by Becquemin et al (1987;1991), Bennett and Zeman (1998), and Schiller-Scotland et al. (1994). These datasets, which provide information for ages 3 months to 21 years, were used for verification of the MPPD model. Figure 11 is the plot of MPPD model predictions against these measurements. Each data point in the figure indicates the predicted deposition fraction against the measured values in a different subject. The age, lung size, and lung breathing parameters were different for each subject. Particle size characteristics were also different in each experiment and were used accordingly to obtain model predictions. In addition, plotted in the figure is the identity line, the line which corresponds to a perfect match between MPPD model predictions and experimental data. The closer the points in Figure 11 to the identity line, the better the agreement between

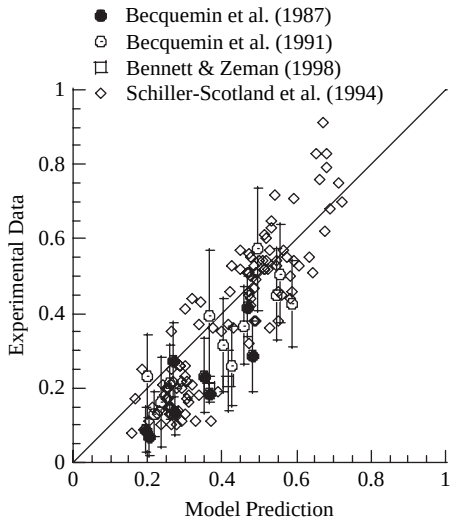

FIG. 11. Comparison of predicted total lung deposition fraction with experimental measurements.

predictions and measurements. Overall, a good comparison between measurements and predictions of lung deposition fraction were observed. However, there was a slight over-prediction of deposition fraction.

Particle deposition models for various ages were exercised across a wide range of particle sizes, with results expressed as % deposition or as deposited dose based upon normalization to lung volume. Predicted particle deposition fractions in the TB region via nasal breathing were almost the same for particles from 0.01 to 2 μm except for 3-month-old infants, where deposition fractions were noticeably higher for particles smaller than 1 (Figure 12A). Due to increased nasal deposition with age (Asgharian et al., 2004), TB deposition was significantly higher in children for fine and coarse PM. Deposition fraction of particles in the alveolar region for all ages showed one peak for particles smaller than 0.1 μm and a second peak for particles larger than 1 μm (Figure 12B). This alveolar deposition pattern appears to be due to the effects of particle filtering in the TB region. Despite having similar shapes, the deposition curves intersected one another, indicating that there was not a clear pattern for deposition fraction with age at a given particle size for these airway geometry models.

Inspection of various parameters controlling particle deposition revealed that differences in lobar deposition depended primarily on lobar volume such that the right middle lobe, which has the least lobar volume, yielded the smallest deposition fraction and lower lobes with greatest volumes were predicted to have the largest deposition. In fact, when adjusted lobar deposition fraction (defined as deposition fraction in a lobe divided by its corresponding lobar volume) was calculated for different particles sizes in all 5 lobes, almost a single functional relationship was observed, indicating similar relative doses among the lobes (Figure 13). In addition, the line representing the ratio of lung deposition fraction to lung volume yielded a similar outcome.

Adjusted lung deposition fraction is a unique feature of the lung for a particular age and thus presents a means for comparing lung dose across age groups. Figure 13 is calculated for an 8-year old but could be estimated for any age group: deposition fraction for different regions of the lung is the same for a given particle size when normalized with the respective volume of the region. Thus, a single deposition curve such as that shown in Figure 13 exists at each age group. This unique feature of the adjusted lung deposition fraction presents a means for comparing lung dose across age groups. Using the MPPD model, Ménache et al. (personal communication; Ashgarian, et al., 2004) calculated deposition fraction per lung volume for different ages and particle diameters between 0.01 and 10 μm. In this modeling framework, a clear pattern with age emerged (Figure 14). At a given particle size, the adjusted lung deposition fraction was highest in infants and decreased with age. The differences in adjusted deposition across ages were related to the differences in lung volume. Due to faster lung growth at

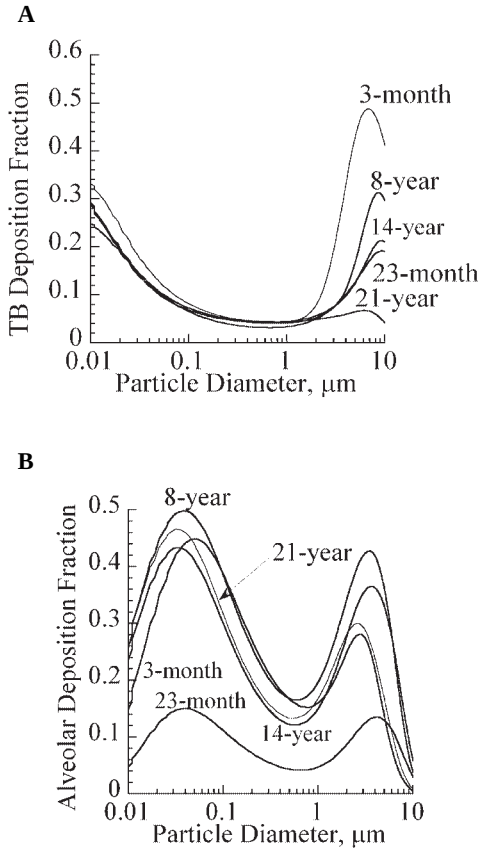

FIG. 12. Age-related mass deposition fraction via nasal breathing predicted as a function of particle size in TB (A) and alveolar (PU) (B) regions by the MPPD model.

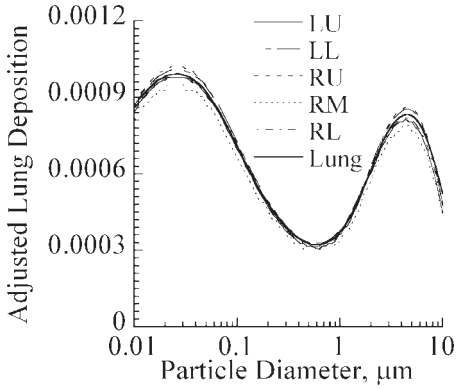

LU = left upper lobe; LL = left lower lobe; RU = right upper lobe; RM = right middle lobe; RL = right lower lobe;

FIG. 13. Adjusted mass deposition fraction of particles predicted by the MPPD model for the entire lung and each lobe of an 8-yr-old child. Deposition fraction values are unitless, adjusted for lung region volume.

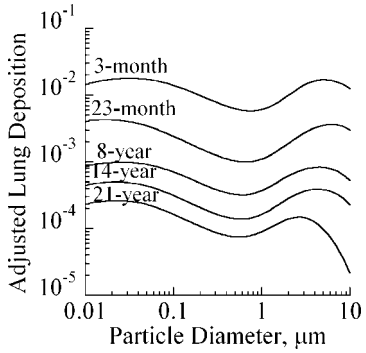

FIG. 14. Adjusted mass deposition fraction in the lungs of children and adults predicted by the MPPD model. Deposition fraction values are unitless, adjusted for lung region volume.

early stages of life, the difference in adjusted deposition was greater in younger ages. The change in adjusted deposition was more gradual after the age of 8 years.

Lung injury is related to local rather than regional deposition. Deposition per surface area is an indicator of local dose. The data in Figure 14 are transformed to be expressed as mass deposition rate per lung surface area in Figure 15. This method of normalization yields a similar trend as the dose/lung volume results, with 3 month-old children having up to an order of magnitude greater deposition dose than adults. This trend occurs at all particle sizes modeled. In each age group, deposited mass per lung surface area is greatest for ultrafine particles, decreases for fine (1 μm) particles and then increases again for coarse particles. Regarding cross-model comparisons, MPPD and ICRP models predict similar regional deposition fractions of various sized particles in adults (Ashgarian, et al., 2001).

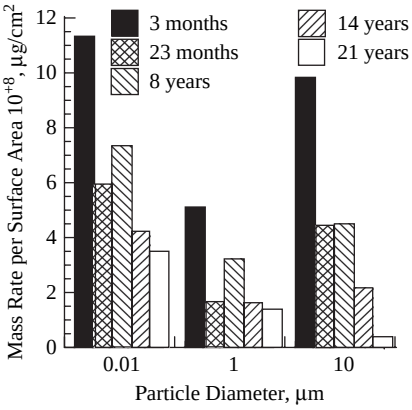

FIG. 15. Particle deposition dose of mass per lung surface area at various ages.

COMMENTS ON PARTICLE CLEARANCE MODELING

Internal doses may be accurately described by particle deposition alone if the particles exert their primary action on the epithelial surface (Dahl et al., 1991). For longer term effects, however, the deposited dose may not be as appropriate because particles clear at various rates from different lung compartments so that some dose is retained (Jarabek et al., 2005). To characterize chronic effects of inhaled particles, models need to calculate retained dose within the respiratory tract by accounting for clearance pathways (U.S. EPA, 1994; 1996; 2004). Recent workshops regarding risk assessment approaches to fiber and particle toxicity recommended that species-specific toxicokinetic models need to be used to predict particle clearance and retention in the lungs (ILSI, 2000; Greim et al, 2001).

Current data gaps necessitate the calculation of deposition and clearance separately in default algorithms, but the two processes are coupled and improved models provide for integrated calculation of retention as the net result of deposition minus clearance (ICRP, 1994; NCRP, 1997). In order to solve for deposition, available mechanistic models idealize the particle transport process by mathematically converting the spread of particles as one-dimensional penetration in the lung and 3-dimensional deposition in airways by various loss mechanisms. In addition, the lung geometry is selected as a dichotomous, symmetric or asymmetric network of cylindrically-shaped airways. Consequently, dose predictions are reliable at the regional level for insoluble PM.

The ICRP respiratory tract dosimetry model accounts for clearance from the respiratory tract as a result of dissolution of particles or elution of their constituents, followed by absorption of the dissolved constituents into cells proximate to the particles, or into the circulatory system for redistribution or excretion. Current efforts by the ICRP are underway to compile these critical data for radiological particles (Bailey et al., 2003). Previous simulation exercises using realistic dissolution-absorption half-times for different PM diameter size modes (fine, intermodal, and coarse) used in support of the NAAQS for PM showed that particle solubility rates are dominant determinants of retained lung burdens of inhaled particles of ambient aerosols (U.S. EPA, 1996; Snipes et al., 1997).

Various assumptions similar to those made for modeling mucociliary clearance in adults are made to estimate the retention of insoluble particle in the conducting airways of the child lung. For example, mucus layer travels at a constant velocity with an effective thickness that is small compared to lumen diameter and mucus production rates are the same in all terminal bronchioles. Since tracheobronchial structure of the lung is complete at birth, modeling of clearance in this region in children generally follows that of adults. Because children have smaller lung geometry, particles have a shorter distance to travel to be cleared and so may be cleared faster than in adults for the same mucous velocity (Figure 16). However, mucous

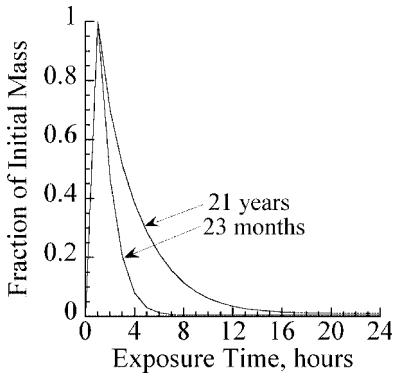

FIG. 16. Simulated fraction of retained mass (unitless) in the TB region of children after a 1-h exposure to 1-μm particles.

velocity is not necessarily constant across age. Wolff (1992) reported the tracheal mucus velocities in beagle dogs at different ages. The data showed that the mucus velocity increased to a maximum value in young adults and then declined with age. He argued that age-related changes in canine lung functions are most similar to those in humans. Thus, mucus velocity in humans may be expected to increase after birth, reach peak values at puberty, and then slowly decrease with age. Clearly, additional detailed information regarding the change in mucus velocity with age is required to realistically estimate the retained dose in the lungs of children.

The MPPD and ICRP models approach clearance in the pulmonary region in an analogous fashion (Jarabek et al., 2005). The clearance model is comprised of fast, medium, and slow compartments to describe the following: macrophage phagocytosis, physical particle translocation on mucociliary escalator, and clearance to the lymph nodes via the alveolar instersitium. The clearance rates used for the fast (γ_{fast}), medium (γ_{med}) and slow (γ_{slow}) compartments were 0.02, 0.001 and 0.0001 /day, respectively. The slow compartment also clears via lymphatic channels (γ_L) at a rate of 0.00002 /day. While the entire pulmonary region is considered as one compartment in the ICRP model, a distinct alveolar compartment distal to each terminal bronchial was assumed in the MPPD model. Accordingly, particle removal from each alveolar (acinar) region was calculated independently. Deposition is then apportioned to the fast (30%), medium (60%), and slow (10%) clearance compartments. This leads to a more accurate characterization of clearance than combining all the alveolar zones into one and then computing clearance for a single alveolar region (Jarabek et al., 2005). Simulation exercises using this model predict a qualitatively similar pattern of retained dose as that of deposited dose in the TB region (Jarabek et al., 2005).

CONCLUSIONS FOR MULTI-PATHWAY PARTICLE DOSIMETRY MODELING

Recent improvements in dosimetry modeling enabled more accurate prediction of deposition of particles in the lungs of adults and children. The models were validated by comparing predicted versus measured deposition in the entire lung of children at different age groups. However, additional morphometric measurements of airway parameters, particularly in the deep lung, are needed to refine these modeling estimates. Further needed are deposition measurements in ET and TB airways across a spectrum of children's ages.

Many childhood lung disorders such as asthma occur in the TB region (Bierbaum and Heinzmann, 2007). Particle deposition and clearance in this region may be crucial to the onset or exacerbation of lung diseases. The current results show that children have the potential for greater total lung mass deposition of a wide range of inhaled PM, but these results need better specification in terms of sub-regions where this across age deposition discrepancy may be greatest. More refined models that are built upon expanded measurements in children are needed to fully understand the implications of this research. Further, particle clearance rates should be included in children's dosimetry models, because of its significant impact on predicted doses. The limitations in mucus-based clearance data are thus another important data gap.

Thus, based on dosimetric considerations, children may face an increased health risk from exposure to airborne PM compared with adults. The risk becomes potentially greater if children are also more sensitive to a given dose of particles due to incomplete development of body defense or repair mechanisms. Improved children's morphologic, deposition and clearance data are needed to improve upon current models.

The particle models presented herein are based on poorly soluble particles. Key physicochemical input parameters are particle diameter and distribution. The exercises presented herein were performed using monodisperse aerosols, but previous simulation exercises demonstrated that consideration of polydisperse exercises influence the predicted deposition and retained dose estimates by at least 2 to 3-fold (U.S. EPA, 1996; Snipes et al., 1997; Jarabek et al., 2005). Evaluation of the influence of polydispersity on predictions for children need to be performed. Other major determinants of deposition and retention such as hygroscopicity (ICRP, 1994; Schroeter et al., 2001) and physical dissolution also need to be simulated in age-appropriate models. Additionally, recent evidence suggests when different types of particles are compared, inhaled dose may be more appropriately expressed as particle volume, particle surface area, or number of particles rather than mass, depending on the adverse effect being evaluated (Oberdörster et al., 1994). Different dose metrics vary both based on whether particle mass or number is used as the internal measure of dose, and on the normalizing factor (e.g., ventilatory units, alveolar units, or alveolar macrophages) (Snipes et al.,

1997; Jarabek et al., 1995). Thus, age-specific data to construct such dose metrics for children are needed.

FACTORS INFLUENCING THE DOSIMETRY OF REACTIVE GASES IN THE LOWER RESPIRATORY TRACT OF CHILDREN

This section focuses on the distribution of reactive gases in the conducting airways (tracheobronchial region) of the LRT. While default models typically divide the airways into a few well-mixed regions and predict the overall extraction of reactive gas in each region, other models such as those used in the regulatory arena for O_3 and formaldehyde describe mass transfer in a more anatomically-accurate lung structure (Miller, et al., 1985; Overton et al., 1987;2001; Weibel, 1963). This section extends the default models by considering the generation-by-generation distribution of reactive gases along a conducting airway path. Simulations are conducted for both adults and children by using age-appropriate breathing and anatomical parameters.

Once distributed by respired air flow among local sites within the lungs, a reactive gas must diffuse through the mucus blanket before it reachs the underlying epithelial cells (Figure 17). Mucus protects these cells by providing substrates that combine with a reactive gas to form benign products. On the other hand, some of the substrates present in mucus might combine with a reactive gas to form secondary toxic products. For example,O_3 is a reactive gas that is detoxified by endogenous antioxidants such as uric and ascorbic acid, but also reacts with polyunsaturated fatty acids to form aldehydes that damage epithelial cell membranes (Bhalla, 1999).

The specific goal of this section was to examine the uptake distribution of gases of different chemical reactivity along the gas-mucus, as well as the mucus-tissue, interfaces in the tracheobronchial tree of children of various ages. The effect of different ventilation rates associated with different levels of physical exertion was also considered. To make the computations concrete, physical-chemical parameter values appropriate for O_3 were employed, including an environmentally-relevant inhaled concentration of 0.1 parts per million by volume (ppm).

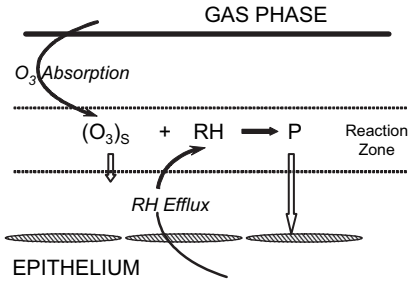

FIG. 17. Diffusion reaction of ozone within the mucous layer. RH=reactive substrate; P=reaction product (may or may not be toxic).

MATHEMATICAL MODEL FOR OZONE UPTAKE IN THE TRACHEOBRONCHIAL REGION

Reactive gas dosimetry was analyzed in a tracheobronchial tree consisting of 15 generations of symmetrically-branched airway bifurcations. This modeling exercise began with air entering the trachea and thus did not simulate reactions possible in the ET region. Each airway was represented by a convection-diffusion model of the gas-filled lumen and a diffusion-reaction model of the surrounding mucus layer (Santiago et al., 2001). The two models were coupled at the air-mucous interface by an overall mass transfer coefficient (Kg) that incorporated the diffusion resistances of both the mucus layer and an adjacent "unstirred" gas layer. The key assumptions were: a steady flow of inspired gas through the airway lumen; and a first-order chemical reaction of the gas within the mucous layer.

Numerical simulations of reactive gas uptake utilized airway parameters specific to children of different ages. The lengths and diameters of airway branches (Table 4) as well as lung ventilation rates (Table 5) were taken from Phalen and associates (1985). The individual mass transfer coefficients for reactive gas transport across the unstirred gas layer (k_g) were computed from one of three established correlations for fully-developed flow through straight tubes (Treybal, 1980). The correlation used in a given situation depended on whether the gas flow was turbulent or laminar and, in the latter case, whether the concentration profile was developing or fully-developed.

It was also necessary to specify parameters within the mucus layer. The liquid-phase diffusion coefficient ($D_m=2.66\times10^{-5}$ cm^2/sec) and the thermodynamic gas-liquid partition coefficient for O_3 ($\lambda = 6.9$) were adopted from the work of Miller and coworkers (1985). The first-order reaction rate constant of O_3 with mucus substrates (k_r) was estimated as 1198 /s employing theoretical computations (Miller et al., 1985), 250,000/ sec from continuous exposure measurements in the nasal cavities (Santiago et al. 2001) and $8x10^6$ /sec from bolus exposure measurements in the lower airways (Bush et al., 2000). A midrange k_r of 10^5 /sec, corresponding to a moderate reaction rate, was employed in most of the analyses in this section. To estimate the mucus thickness (δ) in the airways of different aged children, it was first assumed that the mucus thickness in an adult's lungs declines in a linear fashion from 10 μm in the trachea to 0.1 μm in a 15^{th} generation airway; this is similar to the scheme used by Miller and associates (1985). The mucus thickness in a particular generation of a child's lung was scaled down by the ratio of the child-to-adult airway diameters (Table 6). The individual mass transfer coefficients across the mucus layer (k_m) were then computed using the results of the diffusion-reaction model shown schematically in Figure 18.

TABLE 4
Airway Lengths (L) and Diameters (D) (mm)

	Age (yr)											
	0		4		8		12		16		18	
Gen	L	D	L	D	L	D	L	D	L	D	L	D
0	26.5	5.30	53.5	10.7	65.0	13.0	76.5	15.30	86.50	17.3	89.0	17.8
1	15.8	4.34	25.5	8.06	29.6	9.65	33.7	11.24	37.4	12.6	38.3	13.0
2	5.96	3.28	9.74	5.77	11.4	6.82	13.0	7.88	14.36	8.80	14.7	9.03
3	3.89	2.59	6.75	4.37	7.97	5.13	9.19	5.89	10.25	6.55	10.5	6.71
4	3.71	1.85	5.60	2.77	6.41	3.16	7.21	3.55	7.91	3.89	8.09	3.97
5	2.78	1.41	4.56	2.17	5.32	2.49	6.08	2.81	6.74	3.09	6.91	3.16
6	2.22	1.14	3.41	1.79	3.91	2.07	4.42	2.34	4.86	2.58	4.97	2.64
7	1.98	0.85	2.68	1.22	2.98	1.39	3.28	1.55	3.54	1.69	3.61	1.72
8	1.92	0.70	2.35	0.92	2.54	1.01	2.72	1.10	2.88	1.18	2.92	1.20
9	1.75	0.64	2.24	0.80	2.44	0.87	2.65	0.94	2.83	1.00	2.88	1.01
10	1.64	0.58	2.02	0.69	2.18	0.73	2.34	0.78	2.48	0.82	2.52	0.83
11	1.57	0.51	1.89	0.57	2.03	0.59	2.17	0.61	2.29	0.63	2.32	0.64
12	1.50	0.50	1.77	0.55	1.89	0.57	2.00	0.59	2.10	0.61	2.13	0.61
13	1.43	0.47	1.65	0.50	1.74	0.52	1.83	0.53	1.91	0.54	1.93	0.55
14	1.36	0.45	1.52	0.47	1.59	0.48	1.66	0.49	1.72	0.50	1.74	0.50
15	1.30	0.43	1.41	0.44	1.45	0.44	1.50	0.45	1.54	0.45	1.55	0.45

Note. Source: Computed from the equations of Phalen et al. (1985). Gen=airway generation of a symmetrically bifurcating tracheobronchial tree. Gen 0 is the trachea and Gen 15 corresponds to the terminal bronchioles.

TABLE 5
Ventilation Rates Used in Reactive Gas Modeling

			Minute volume (L)		
Age (yr)	Weight (kg)	Height (cm)	Quiet breathing	Light exertion	Heavy exertion
0	3.3	50	1.52	3.00	8.92
4	16.4	104	3.18	6.34	19.00
8	27.0	127	4.53	9.05	27.10
12	43.0	150	6.56	13.10	39.30
16	63.0	170	9.10	18.20	54.60
18	70.0	175	10.0	20.0	60.0

Note. Source: Phalen *et al.* (1985).

The overall mass transfer coefficient for the unstirred gas and mucus layers was computed by combining the individual mass transfer coefficients (Treybal, 1980).

$$Kg = (1/k_g + 1/k_m)^{-1}$$

The final results for Kg during quiet breathing for a gas with a moderate reactivity of $k_r=10^5$ /sec is shown in Table 7. in addition, shown in this table is % overall diffusion resistance that is attributable to the mucus layer. Notice that for all ages and all airways, the controlling resistance for reactive gas uptake is in the mucus layer rather than in the unstirred layer of the respired air.

RESULTS FOR LRT MODEL OF OZONE UPTAKE

Figures 19 through 21 demonstrate how the flux of O_3 (*i.e.*, amount absorbed per unit time per unit surface area) varies from generation to generation along the gas-mucous interface

TABLE 6
Mucous Thickness (μm) Scaled From Adults by Relative Airway Diameter

	Age (yr)					
Gen	0	4	8	12	16	18
0	2.98	6.01	7.30	8.60	9.72	10.00
1	2.34	4.35	5.20	6.06	6.80	6.99
2	1.69	2.98	3.52	4.07	4.54	4.66
3	1.28	2.16	2.53	2.91	3.23	3.31
4	0.87	1.30	1.49	1.67	1.83	1.87
5	0.63	0.97	1.11	1.26	1.38	1.42
6	0.49	0.76	0.88	1.00	1.10	1.12
7	0.34	0.49	0.56	0.62	0.68	0.69
8	0.27	0.35	0.38	0.42	0.45	0.46
9	0.23	0.29	0.31	0.33	0.36	0.36
10	0.19	0.23	0.24	0.26	0.27	0.28
11	0.16	0.18	0.18	0.19	0.20	0.20
12	0.14	0.16	0.16	0.17	0.17	0.18
13	0.12	0.13	0.14	0.14	0.14	0.14
14	0.11	0.11	0.12	0.12	0.12	0.12
15	0.09	0.10	0.10	0.10	0.10	0.10

Note. Gen=airway generation of a symmetrically bifurcating tracheobronchial tree. Gen 0 is the trachea and Gen 15 corresponds to the terminal bronchioles.In the 18-yr-old lung, mucous thickness decreased in a linear fashion from 0.1 μm in Gen 0 to 0.1 in Gen 15 (Miller et al., 1985). For younger lungs, the mucous thickness in a given Gen was scaled down by the ratio of the airway diameter in the young lung to the airway diameter in the same Gen of the 18-yr-old lung.

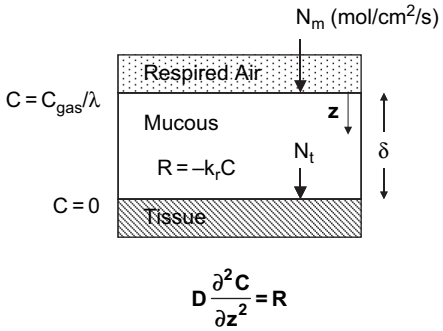

FIG. 18. Diffusion-reaction model of gas transport in the mucous layer. In this quasi-steady-state model, diffusion $D(\partial^2 C/\partial z^2)$ is balanced by the first-order reaction rate *R* of reactive gas with endogenous substrates. Nm is the overall flux of reactive gas into the mucous layer, whereas Nt is the flux reaching the epithelial surface.

(N_m) and along the mucus-tissue interface (N_t) when a constant concentration of 0.1 ppm is inhaled.

Figure 19 illustrates the sensitivity of N_m and N_t to the reactivity of the gas in mucous (k_r). For highly reactive gases (bottom panel), N_m is substantial in the proximal conducting airways where most of the gas is scrubbed out of the airstream, analogous to what happens in the ET region in models where this compartment is present. Flux into the tissue (N_t) is negligible in all the conducting airways since the gas is so reactive in the mucus layer. For slowly reacting gases (top panel), the N_m and N_t distributions are quite similar, with a clear maximum in dose appearing at an intermediate airway generation. For moderately reacting gases (middle panel), the N_m distribution was similar to that observed for highly reactive gases, while the N_t distribution was similar to that observed for slowly reacting gases.

Figure 20, produced for a moderately reacting gas, illustrates the effect of different ventilation rates imposed by different levels of exertion. As exertion increases, the magnitudes of N_m and the peak values of N_t rise. Figure 21 illustrates the effect of age during quiet breathing. As age increases, the longitudinal distributions of both N_m and N_t shift distally toward the respiratory airspaces.

DISCUSSION OF RESULTS FOR OZONE UPTAKE IN THE LRT

Assuming a moderate reaction rate, virtually all of the O_3 inhaled by children 0–8 years old was absorbed in the mucus lining layer of the tracheobronchial tree during quiet breathing (N_t falls to 0 in the terminal airway generation). When gases have a lower reactivity or breathing occurs at higher ventilation rates, less gas is extracted by the mucus layer so that more gas penetrates to the respiratory airspaces. Increased penetration of O_3 to the respiratory zone also occurs as an individual ages beyond 8 years. Because the overall mass transfer coefficient is not sensitive to age (Table 7), this must be attributed to the increase in the ventilation rate and decrease in the airway surface-to-volume ratio that occurs with aging.

Under all circumstances, increasing the assumed reactivity resulted in a higher O_3 dose to the mucus surface but a lower O_3 dose to the underlying tissue. If all the products of O_3-substrate reactions were non-toxic, this suggests that a rapidly-reacting gas might produce less tissue damage than a slowly-reacting gas. However, if the reaction products were toxic, then the entire flux of reactive gas across the mucus surface may result in tissue damage, and a rapidly-reacting gas might produce as much tissue damage as a slowly-reacting gas.

The shapes of the uptake distributions suggest that there are focal regions where tissue damage occurs. Longitudinal hot spots of N_t appeared in the distal portion of the conducting airways when low to moderate chemical reactivity was assumed. Similarly, N_m exhibited peak values under several circumstances. The magnitudes of these peaks were affected by ventilation rate but were not particularly sensitive to age.

Although the physicochemical parameters used in the analysis were appropriate for O_3, other gases would behave in a qualitatively similar way. The diffusion coefficient for O_3 is, in

TABLE 7
Estimated Overall Mass Transfer Coefficient K_g (cm/s) and Percent of the Overall Diffusion Resistance Due to the Mucous Layer (%) for the Conditions of Figure 20

	Age (yr)											
	0		4		8		12		16		18	
Gen	K_g	%	K_g	%	K_g	%	K_g	%	K_g	%	K_g	%
0	0.217	92	0.201	85	0.197	83	0.193	82	0.192	81	0.191	81
1	0.220	93	0.209	88	0.206	87	0.204	86	0.203	86	0.203	86
2	0.225	95	0.218	92	0.216	91	0.215	91	0.214	91	0.214	91
3	0.226	96	0.221	93	0.219	93	0.218	92	0.217	92	0.217	92
4	0.227	96	0.224	95	0.224	95	0.223	94	0.223	94	0.223	94
5	0.229	97	0.225	95	0.224	95	0.224	95	0.224	95	0.224	95
6	0.230	97	0.226	96	0.225	95	0.225	95	0.224	95	0.224	95
7	0.236	97	0.229	96	0.228	96	0.228	96	0.227	96	0.227	96
8	0.248	97	0.235	97	0.232	96	0.231	97	0.231	97	0.231	97
9	0.260	97	0.242	97	0.238	96	0.236	96	0.234	96	0.233	96
10	0.278	97	0.259	97	0.252	97	0.248	97	0.245	97	0.244	97
11	0.307	97	0.290	97	0.284	97	0.279	97	0.275	97	0.273	97
12	0.326	97	0.308	97	0.301	97	0.295	97	0.291	97	0.290	97
13	0.357	97	0.341	97	0.335	97	0.329	97	0.324	97	0.323	97
14	0.393	97	0.379	97	0.374	97	0.369	97	0.364	97	0.363	97
15	0.439	97	0.430	97	0.426	97	0.423	97	0.420	97	0.419	97

Note. K_g computed from individual gas and liquid phase coefficients as suggested by Treybal (1980). Gen=airway generation of a symmetrically bifurcating tracheobronchial tree. Gen 0 is the trachea and Gen 15 corresponds to the terminal bronchioles.

fact, similar to other reactive gases of environmental concern. O_3 is sparingly soluble, however, and highly soluble/reactive gases such as chlorine and formaldehyde would undoubtedly be absorbed more in the URT and more proximally in the lungs.

It is important to point out the limitations associated with the current work. First, although this analysis focused on the tracheobronchial tree, the upper airways remove a substantial amount of inhaled reactive gas before it reaches the lower airways. Second, the airway lumen model only incorporates uptake during steady state inspiratory flow. Thus, it does not consider uptake during expiration and can not account for the effects of tidal volume or breathing frequency. Third, because the reaction rate of the inhaled gas is assumed to be first order, the mucus layer model can not accommodate situations where the availability of substrate becomes a limiting factor in the diffusion-reaction process. Fourth, the use of mass transfer correlations for straight tube flow only provides a rough approximation of the convective-diffusion occurring in the lumen of bifurcating airway branches. Fifth, the estimates of mucus thickness as a function of age were rudimentary. It was assumed that mucus thickness scales with airway diameter when it may really depend on other factors more closely associated with the dynamics of the mucociliary system. Finally, our simulations on a specific airway model were completed based on a limited number of airway casts (Phalen, et al., 1985).

In spite of these limitations, the analysis revealed some important trends in the uptake distribution of a reactive gas. Under the current assumptions of anatomy and air flow, children do not appear to receive markedly different mucus or tissue flux than adults. Critical gaps remain to be filled, such as our knowledge of chemical reaction rates and mucus thicknesses in the developing lung.

NASAL IMAGING AND COMPUTATIONAL FLUID DYNAMICS-BASED DOSIMETRY MODELS TO REFINE RISK ASSESSMENTS FOR CHILDREN

Refining children's inhalation dosimetry estimates will be aided by models that simulate air flow based upon detailed three dimensional (3D) anatomical descriptions of the airways. Computational fluid dynamic (CFD) models were developed as a tool to explore respiratory tract deposition of particles and aerosols in lab animals and adult humans, but efforts to adapt this methodology to children is just beginning. This section describes some of the current applications of CFD modeling and its potential to inform risk assessment for children.

CFD models are composed of an anatomically-accurate grid or mesh of the airways that is used to solve the equations of inhaled air and material transport as shown for the URT in Figure 22. These solutions allow prediction of localized dose

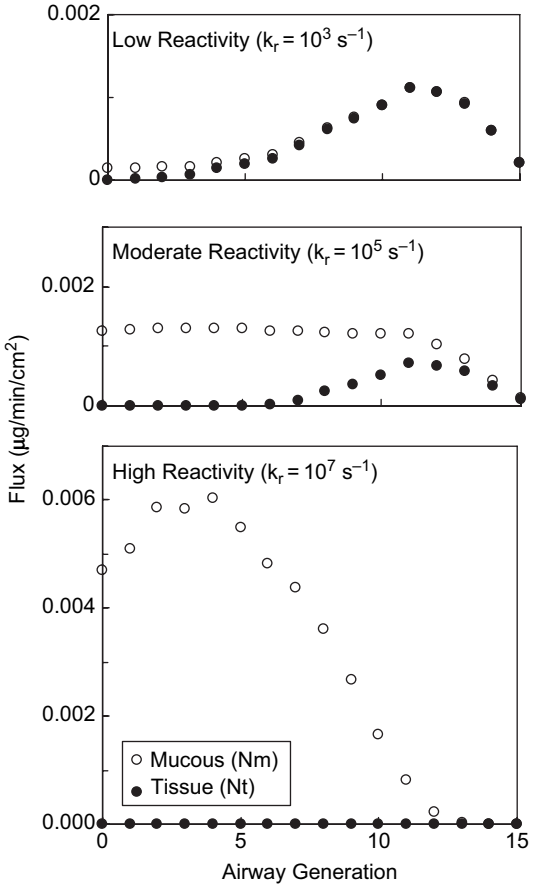

FIG. 19. Prediction of flux to the lower respiratory tract for an 8-yr-old inhaling 0.1 ppm of a gas of varying reactivities under quiet breathing conditions.

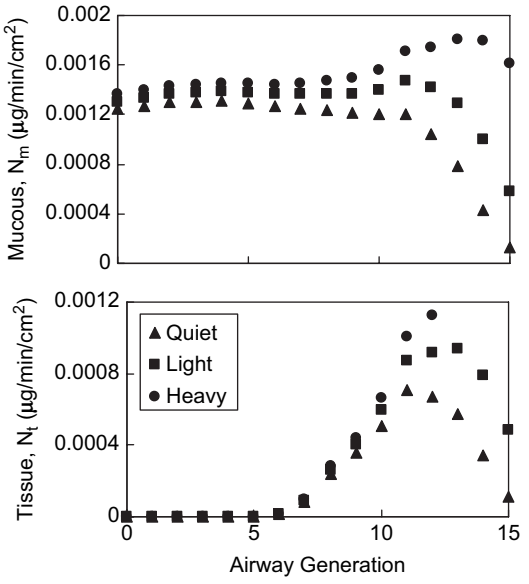

FIG. 20. Estimates of ozone flux to the lower respiratory tract for an 8-yr-old inhaling 0.1 ppm O_3 at various activity levels (Table 5) assuming a moderate reactivity with mucous (k_r=10^5 s^{-1}).

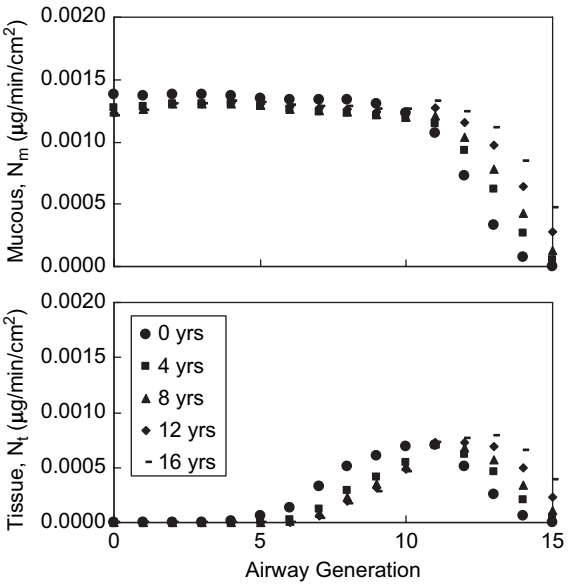

FIG. 21. Flux of ozone to mucus (top panel) and tissue (bottom panel) predicted for children of different ages inhaling 0.1 ppm O_3 during quiet breathing. Assumption of moderate reactivity with mucous (k_r=10^5 s^{-1}).

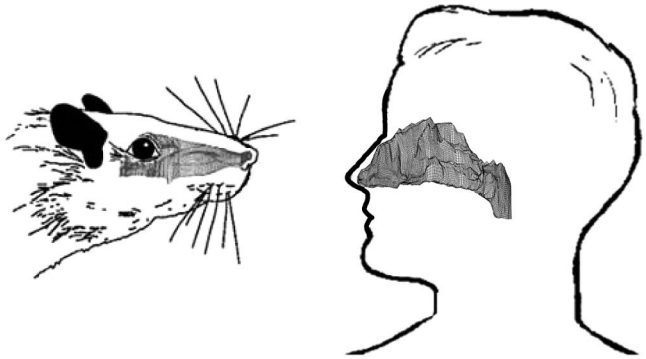

FIG. 22. Lateral views of the three-dimensional meshes from computational fluid dynamics (CFD) models of the nasal passages of an adult male rat (left) and human (right). (Head outlines provided for reference.)

of inhaled material to airway walls (Kimbell et al., 2001a; Moulin, et al., 2002). CFD airway geometry is usually derived from computer-aided tomography (CT) scans, magnetic resonance imaging (MRI) scans, or digital photographs of microscope slides or sectioned specimens. The description of the walls of the CFD model includes spatial information on the distribution of epithelial types and metabolic activity. This information influences the predicted uptake and distribution of inhaled material and aids in interpreting modeling results. The CFD model may also be linked to a physiologically-based pharmacokinetic (PBPK) model of tissue disposition if the

mode of action suggests that including this detail is necessary for accurate prediction of the dose associated with important toxicity. PBPK models typically represent regions of the body as well-mixed compartments based on regional air and tissue volumes and may also encode information on biochemistry, metabolism, and the flows of air, blood and other body fluids to predict dose within compartments.

CFD models of the nasal passages were linked to PBPK or other dosimetry models in three ways. First, a CFD model for air-phase transport provides input to a PBPK model for tissue transport (Figure 23A). An example of this type of linkage is the estimation of formaldehyde-induced DNA-protein cross links (DPX) in the rat and human nasal passages. Here CFD models were used to predict regional wall mass fluxes of formaldehyde. These predicted fluxes were used as inputs to PBPK models that in turn predicted DPX formation (Cohen Hubal et al., 1997; Conolly et al., 2000). Nasal CFD uptake predictions were also used to calibrate the estimated flux from the nasal compartment to the lower regions of single-path mass transfer models of the entire respiratory tract at different flow rates. The calibrated respiratory tract model was used to predict formaldehyde uptake in the human lungs for various activity patterns (Overton et al., 2001).

Second, CFD models were used to provide some of the parameter values of a PBPK model (Figure 23B). Examples of such CFD-informed PBPK models include the transport of acidic vapors (Frederick et al., 1998) and methyl methacrylate (Andersen et al., 1999). In these models, CFD-derived air-phase mass transfer coefficients that estimate the amount of resistance encountered by a gas as it passes from the bulk airstream to the airway walls were incorporated into the transport process from air to tissue compartments. Third, PBPK models are used to optimize parameters that are then used in the airway wall boundary conditions of CFD models

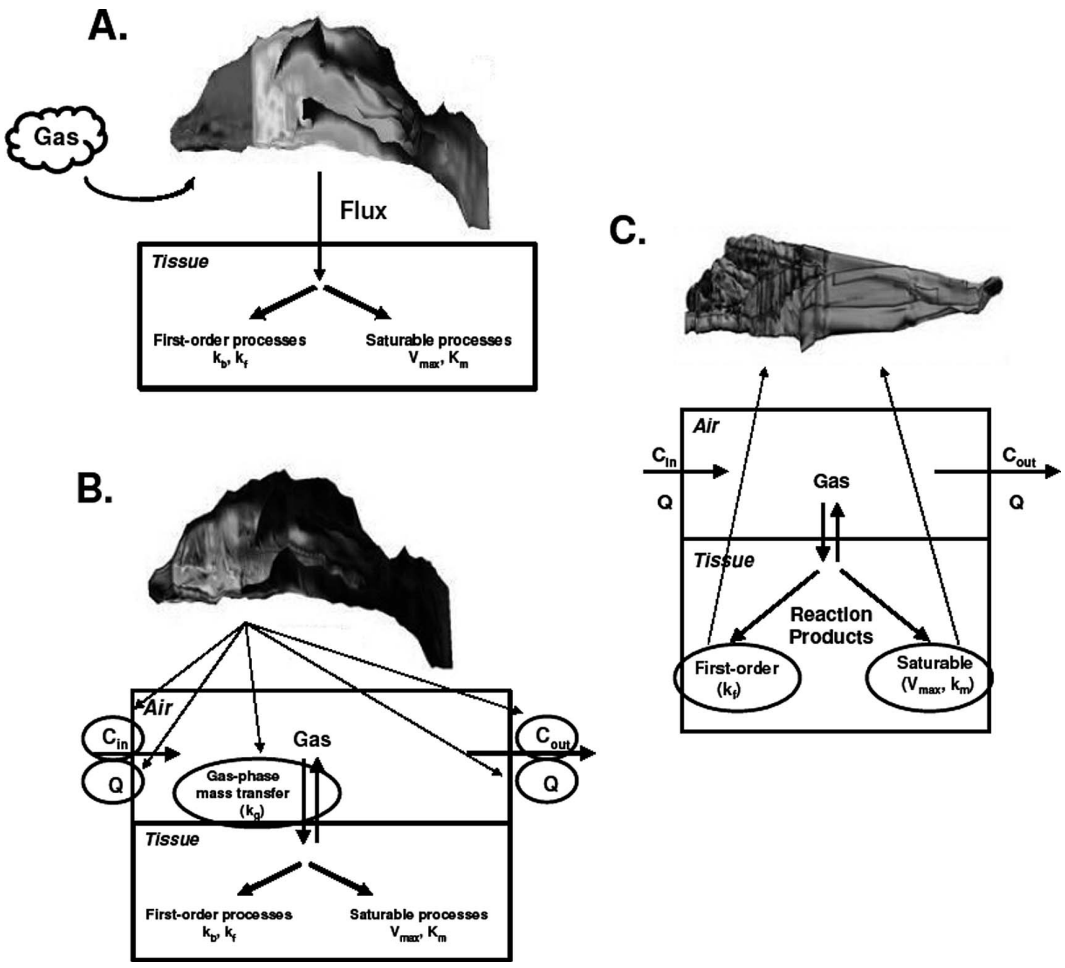

FIG. 23. Linkages between CFD and PBPK models. (A) CFD model predicts flux of inhaled material from the air-phase directly into a PBPK model for tissue transport. (B) CFD model is used to calculate parameter values that are then used in a PBPK model. (C) PBPK model of a rat is fitted to nasal extraction measurements to optimize the values of parameters that are then used in the airway wall boundary conditions of a rat nasal CFD simulation.

(Figure 6–2C). The model for hydrogen sulfide transport developed by Schroeter and colleagues (2006a;2006b) is an example of a PBPK-informed CFD model. First-order and saturable metabolic parameters were obtained by fitting a PBPK model for nasal extraction of hydrogen sulfide to data measured in rats. The fitted parameters were then incorporated into the airway wall boundary conditions of a CFD model for hydrogen sulfide transport in the air phase so that localized wall mass flux predictions could be compared with lesion distribution data. Nasal CFD models were created for many species including frogs, rats, rabbits, horses, monkeys, and adult humans.

Figure 24 shows how different types of anatomical information were used as the basis of CFD models for rats, monkeys and humans. The CFD model develops airflow patterns from the anatomical mesh, and when combined with mathematical descriptions of boundary conditions (air/mucus interface) and chemical-specific diffusivity and mass transfer coefficients, leads to estimates of gas uptake and particle deposition (Figure 25). Nasal CFD models are useful in risk assessment for testing hypotheses about dominant mechanisms of toxicity (Hotchkiss et al., 1994; Cohen Hubal et al., 1996; Kimbell et al., 1997; Moulin et al., 2002; Schroeter et al., 2006a), for extrapolating tissue responses in lab animals to individuals on the basis of tissue dose (Conolly et al., 2000;2002;2004; Kimbell et al., 2001b; Schroeter et al., 2006b), and for exploring effects of interindividual variability in nasal geometry on dose among adult humans (Segal et al., 2004; Kimbell et al., 2005a). The need to include children in the study of inter-human dose variability has motivated the extension of nasal imaging-based modeling to early life stages.

A first attempt to incorporate age-specific anatomical and breathing parameters into 3D nasal dosimetry was made by scaling an adult nasal CFD model by nasal volume to represent other age categories (Kimbell et al., 2005b). In this study, age-specific ventilation rates for various activity states and hr/day in the activity (Table 8) were used to predict localized nasal uptake of inhaled formaldehyde for 5 age groups: 3 months, 1 year, 5 years, 10 years, and 15 years old. Together with formaldehyde uptake predictions for age-specific lung generations and activity pattern information, these results will be used in a clonal growth model for formaldehyde carcinogenesis to estimate lifetime cancer risks and compared with lifetime risk estimates that were based on adult dosimetry predictions for all life stages.

Improvements in CT and MRI scanning technologies made it possible to make high-resolution images of the nasal passages of children on which CFD models for children's nasal dosimetry models may be based (Figure 26). However, scans are relatively rare in children, especially infants, and archived scans are often of low resolution and thus of limited utility.

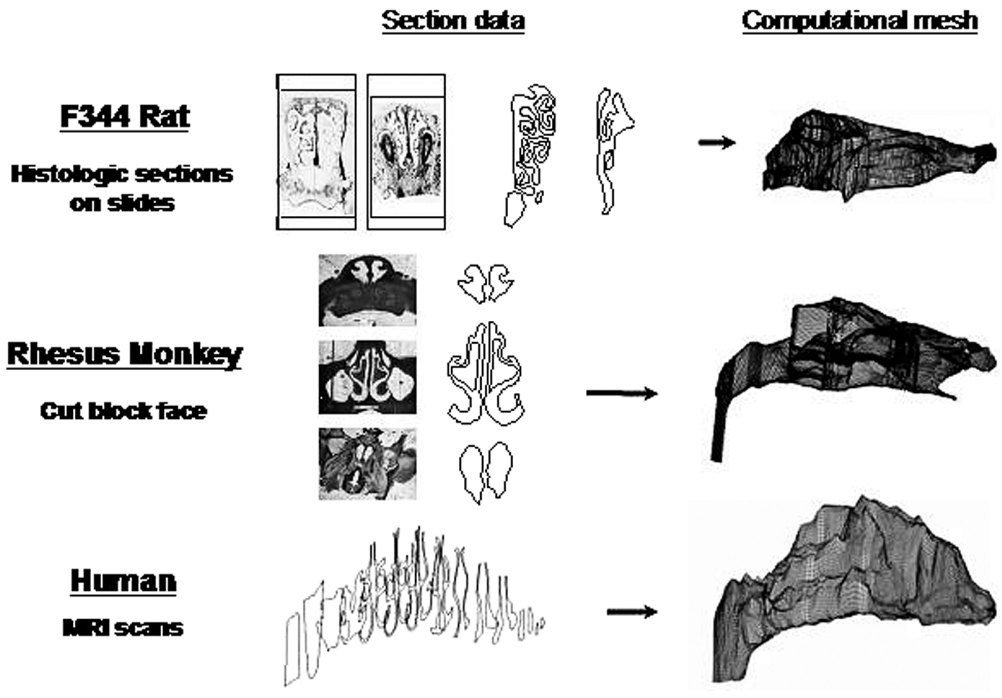

FIG. 24. Nasal CFD model construction. Examples of anatomical data upon which nasal CFD models have been based. For the rat and monkey nasal models shown here, airway outlines on slides of tissue sections (rats) or tissue block faces (monkey) were photographed and processed by hand-tracing (rat) or image analysis (monkey). For the human model shown here, MRI or CT images were used. New imaging technologies are making MRI and CT images possible even for the small, intricate nasal passages of mice and rats. Modified from Kimbell (2006).

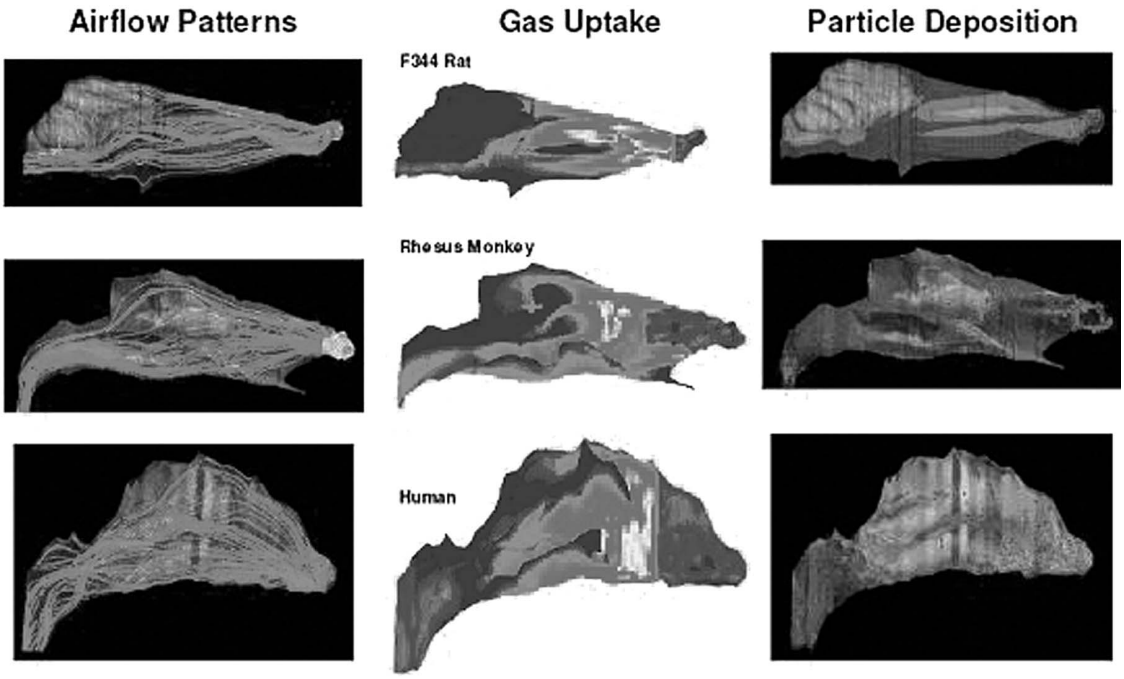

FIG. 25. CFD dosimetry computation. Examples of CFD modeling results. Predicted patterns of inspiratory airflow are illustrated by streamlines (left panels). Regional predictions of inhaled formaldehyde uptake (Kimbell et al., 2001a) show highly nonuniform patterns (center panels; red indicates high uptake rates; blue indicates low uptake rates; reprinted from Kimbell et al. (2001a) with permission from Oxford University Press. Estimates of localized nasal particle deposition can aid understanding of interspecies differences in responses to particle exposure (right panels; modified from Kimbell (2006).

TABLE 8
Age-Specific Activity Patterns Used in CFD Modeling of Formaldehyde Deposition

	Sleeping		Sitting		Light exercise		Heavy exercise	
Age	V_E (L/min)	h/d	V_E (L/min)	h/d	V_E (L/min)	h/d	V_E (L/min)	h/d
3 mo	1.5	17			3.2	7	NA	NA
1 yr	2.5	14	3.7	5	5.8	5	NA	NA
5 yr	4.0	12	5.3	3	9.5	6	37.0	3
10 yr	7.0	10	8.0	3	23.0	8	48.7	3
15 yr	7.5	10	9.0	4	25.0	7	50.0	3
Adult[b](not at work)	7.5	8[a]	9.0	8[a]	25.0	8[a]	NA	NA
Adult(light work)	7.5	8[a]	9.0	6[a]	25.0	9[a]	50.0	1[a]
Adult(heavy work)	7.5	8[a]	9.0	4[a]	25.0	10[a]	50.0	2[a]

Note. Source: ICRP (1994). = minute ventilation (cyclic breathing). NA=not applicable.
[a]Adult is defined as male at 21 yr.
[b]Conolly et al. (2004), based on ICRP (1994).

Improved imaging data for children's nasal airways is critical for developing a reliable CFD approach for predicting toxicant uptake evaluating inter-individual variability.

Advances in imaging technology and CFD model construction are leading the way toward more complete anatomical descriptions and models of the entire respiratory tract (Corley et al., 2006). Ongoing work in 3 and 6-month old non-human primates involves the development of 3D reconstructions of lung and nasal airways to enable localized analysis of O_3 dose (Carey et al., 2007). The deposition patterns obtained from this

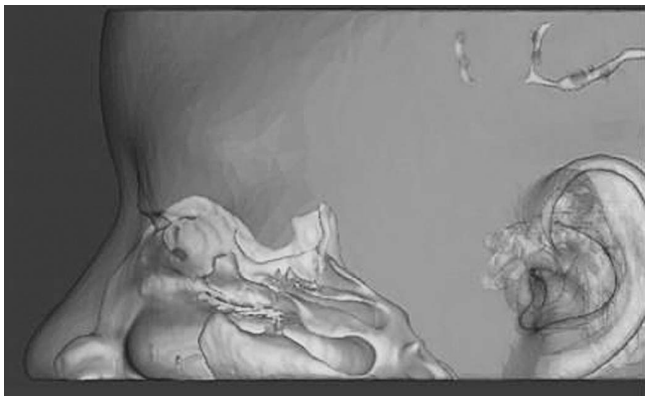

FIG. 26. A three-dimensional reconstruction from CT scans of the outer head and nasal passages of a 14-yr-old human female.

modeling will be used to predict the main loci of ozone injury and help understand the effects of air pollution on the developing respiratory tract. Scanning anatomical data in humans of different ages would enable model extrapolation of dose response seen in animals to humans.

The development of children's CFD models will allow us to (1) make localized predictions of dosimeters, (2) study the effects of interindividual variation in anatomy and breathing parameters, and (3) make direct comparisons of dose among species and life stages. The combined CFD/PBPK modeling approach that has been successful for prediction of adult inhalation dosimetry will have similar advantages in children: multiscale levels of dose resolution including cellular, organ and system levels, and the ability to base risk estimates on relevant, species-specific dose predictions for dose metrics motivated by the mode of action. Combined with increased information on anatomical and metabolic data for children's respiratory tracts such as mucus and tissue thicknesses, cell type and enzyme activity distributions, and localized blood flow and biochemical reaction rates, image-based CFD/PBPK modeling will significantly improve the scientific basis for accurate inhalation risk estimation in children.

DECISION ANALYSIS FRAMEWORK FOR COMPARING DOSIMETRY MODELS

Both the fact that this workshop was convened, and a review of the topics covered, demonstrate that advances in biotechnology drive regulatory authorities such as the U.S. EPA to keep risk assessment approaches contemporary with the state of the science. To do so, the goal of regulatory risk assessment is to integrate diverse types of data now becoming available (e.g., functional genomics) with established outcome measures of adverse health effect, typically endpoints observed at the population (e.g., mortality and morbidity), target tissue (e.g., organ histopathology), or subcellular levels (e.g., clinical chemistry). The challenge to integration will be to rectify these observations at the more microscopic level of organization with traditional default notions about the shape of the dose-response relationship and to appropriately modify approaches for dosimetry descriptions and associated interspecies and intrahuman variability. For example, the U.S. EPA has revised its cancer risk assessment guidelines to emphasize the use of as much mechanistic data as possible to identify the mode of action (MOA), defined as the influence of a chemical on molecular, cellular and physiological functions, in producing toxicity (U.S. EPA, 2005).

However, the characterization of the MOA and estimation of risks to children from air pollutants is complicated by the lack of reliable age-specific epidemiological data. Extrapolations from adults or lab animals present significant challenges: (1) differences in the MOA due to pharmacokinetic (PK) or pharmacodynamic (PD) differences; (2) integration of data ranging from *in vitro* biochemical to population studies; and (3) analysis of the quality and reliability of predictions. As discussed in the introduction, risk assessment approaches address these issues in a somewhat piecemeal fashion, ranging from default UF for interspecies and intrahuman variability to the use of mechanistic models. Pharmacokinetic (PK) and PD data are being developed for different life stages in lab animals and biomonitoring advances may provide measurements directly in humans (both adults and children). While these new technologies bring MOA data to bear on extrapolations, the problem of comparing disparate models that may use the same or different aspects of the information remains. For example, one dosimetry model may have a different range than another (e.g., see Section 3 for particle dosimetry models). As another example, one dosimetry model may empirically estimate age-specific doses at the population level while another predicts doses at the tissue level using mechanistic descriptions of processes believed to be involved. This latter case is essentially the difference illustrated for modeling reactive gas uptake between the default "rudimentary" predictions of parent uptake described in Section 3 versus calculations of tissue dose metrics described in Sections 4 and 5. Often when evaluations of models are made it is not recognized that different dose metrics are being compared.

Ultimately a synthesis of diverse data in needed to arrive at decisions regarding (in the case of our specific application here) the utility of a dosimetry model structure to provide a dose estimate for use in dose-response analysis. This has placed emphasis on arriving at decisions in a rational and reliable manner (National Research Council, 1994). Decision analysis tools are proving useful to articulate principles underlying MOA in order to formalize an approach that may be used to judge the rationality and reliability of different model structures. This judgment is within the broad arena of how the resultant risk estimates from a model are to be used or applied under the different conditions required by regulatory risk assessment (Jarabek and Crawford-Brown, personal communication). Considering the target context of a specific model

(e.g., gas uptake in the URT of a 10-year old child) is a critical part of ascertaining whether various premises and parameters used in a model represent an appropriate means to reach the end application. That is, systematic comparison of competing models, their resultant estimates, and their epistemic status (i.e., degree of evidential support) must be done relative the decisions being made based on their application (e.g., screening versus health standard promulgation). A key criterion for constructing this target context is to also acknowledge that it must be an iterative process to allow advances in interpretation and application to evolve with the state of the science, indeed the very motivation for using decision analysis.

The decision analytic framework is proposed to (1) systematically analyze and compare model structures; (2) evaluate data interpretation, integration, and reliability; (3) assess valuation of parameters; and (4) rationally assess the quality of resulting model predictions (Jarabek and Crawford-Brown, personal communication). The proposed approach first develops a conceptual model to identify both the process of interest and the target context (e.g., reactive gas uptake in nasal tissue of 10-year old children). The next step is to identify key parameters involved in calculations that take a given exposure to a dose metric deemed relevant to the process (e.g., gas concentration, ventilation rate, mass transfer, and flux to specific airway epithelium). After identification, the next step is to determine the quality and relevance of the data, parameter values, and extrapolation premises used to support a given model structure and predictions. Issues of data reliability (the extent to which the evidence can be used to form an inference) and relevance (the extent to which the evidence has the tendency to make a fact probable within the context of a specific judgment being formed) represent theoretical concepts relating to the degree of evidentiary support or the level of proof. An important aspect in the approach is that this level of proof may be different as one extends the dose description to different levels of organization.

Criteria to assess these judgments, premises, and parameters are different for different categories of evidence (e.g., direct empirical or theory-based inference) and are listed in Table 9 (Bunge, 1987). These 7 principles are then combined into an application for rational risk analysis (Crawford-Brown, 2005). The framework then assesses the rationality of predictions of the process in a target context (human children), including evaluation of the strengths and weaknesses of alternative parameters and model forms, the reliability of resulting risk estimates, and key sources of residual uncertainty. Such an analysis would be transparent to external scrutiny and show how conclusions follow deductively from premises. The premises are examined for uncertainty and how they propagate through to uncertainty in resultant conclusions. Rational strategies are formalized most clearly by logic trees or inference frameworks, and the steps in the framework are shown schematically in Figure 27 (Jarabek and Crawford-Brown, personal communication). If needed for the application, a formal uncertainty analysis is facilitated by this analysis tree.

TABLE 9
Principles of Rationality

- Conceptual clarity: Terms are rigorously defined and agreed upon by the relevant community.
- Logical consistency: Predictions or estimates follow deductively from assumptions made and the data used.
- Ontological soundness: Terms appearing in an analysis conform to scientific understanding of the phenomenon (e.g., mass transfer) in question.
- Epistemiological reflection: Assumptions used are subject to scrutiny to determine degree of evidential support.
- Methodological rigor: Use of clearly defined methods that have proven reliable in past applications.
- Practicality: Methods can be completed in a reasonable length of time and with reasonable resources.
- Valuational selection: Attention is focused on values deemed most important.

Note. Source: Bunge (1987).

Using the decision approach to compare model structures developed to address children's risk will aid their systematic evaluation. Because the process diagrams show the flow of information to arrive at a decision, issues of reliability regarding premises are readily revealed. Critical parameter values that may need more data are also easily pointed out.

SESSION SUMMARY: APPLYING CHILDREN'S INHALATION DOSIMETRY MODELING IN HUMAN HEALTH RISK ASSESSMENT

The model structures and simulations presented in this session of the workshop covered a wide range of inhaled materials (ultra-fine, fine, and coarse particles; reactive to non-reactive gases), age groups (3 months to adult), and modeling types (default to data-intensive CFD models). Despite limitations in available age-specific data, the overall conclusion is that there are important anatomical and physiological differences between young children and adults that may lead to important differences in internal dose of these inhaled materials. Differences in delivered dose may account for observed differences in susceptibility of children versus adults (Bobak and Leon, 1999; Gent, et al. 2003). This may be especially true for particle deposition in the lower respiratory tract where an increased dose relative to adults may lead to enhanced adverse pulmonary effects and mortality in children (Bobak and Leon, 1999). Thus, factors that determine inhalation dosimetry need to be

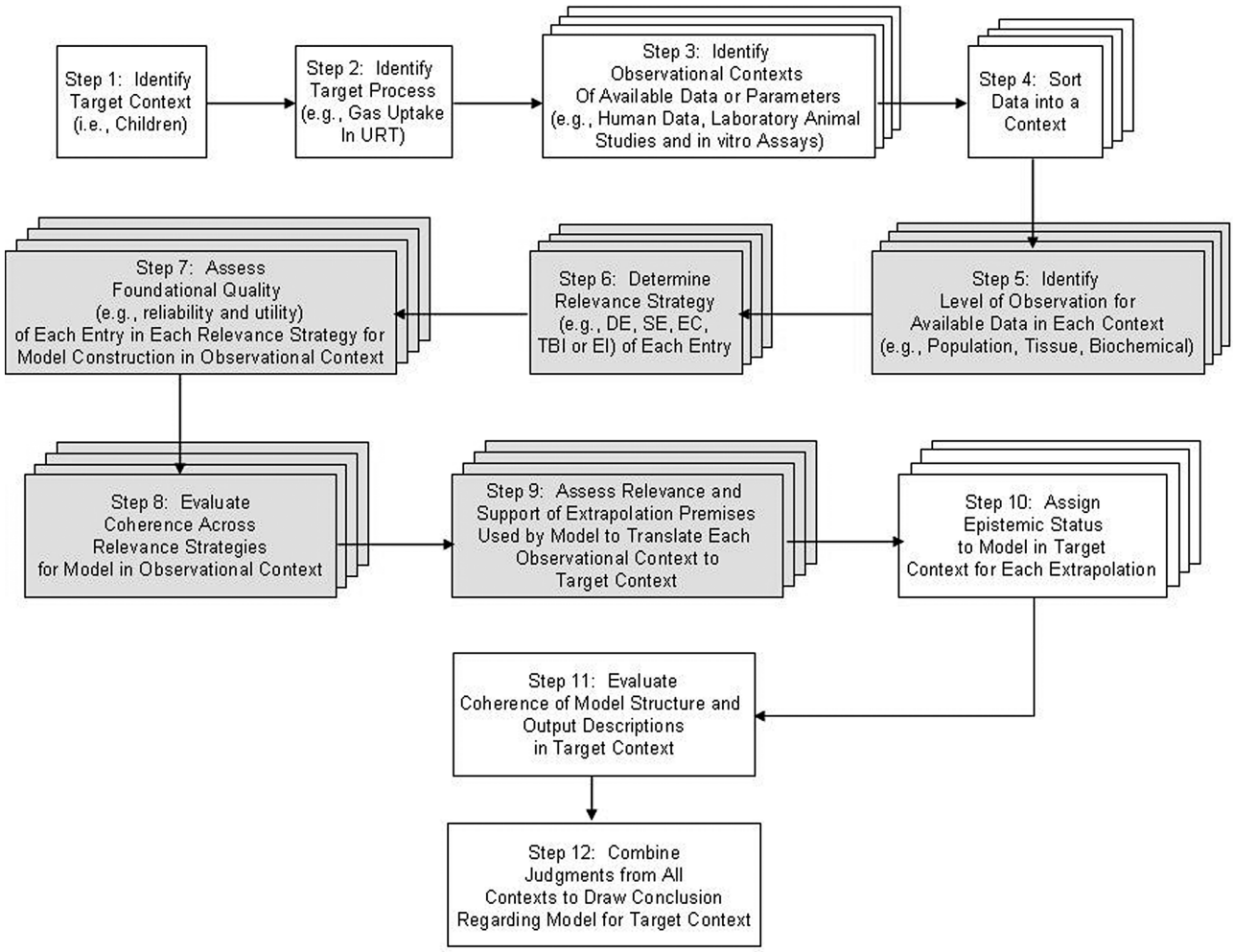

FIG. 27. Schematic of general steps involved in a rational decision analysis for comparison of different dosimetry model structures. The stacked boxes indicate different observation contexts (e.g., different laboratory or species). The shaded boxes denote where data may need to be considered at various levels of observation (e.g., target tissue, cellular, and biochemical) and different dose descriptions may occur at each level. Relevance strategies (evidence categories) listed in step 4 are depicted as DE=direct empirical, SE=semiempirical, EC=empiric correlation, TBI=theory-based inference, and EI=existential insight. Adapted from Crawford-Brown (1999) and Jarabek and Crawford-Brown (personal communication).

considered in addition to behavioral factors (time spent in physical exertion/play activities, location of these activities) in order to refine estimates for human risk assessments of inhaled materials.

However, children's inhalation dosimetry is not typically estimated or taken into account in risk assessment of inhaled agents. As described in the summary for Session 1 of this same workshop (Foos et al., 2007), data available in some risk assessment processes, such as promulgation of the National Ambient Air Quality Standards (NAAQS), may allow evaluation of children's risk directly. However, in most cases, lab animal data are extrapolated to estimate human health risk. Some approaches that rely on lab animal data do not provide for inhalation dosimetry adjustment to arrive at human estimates, while approaches such as the RfC methods which do apply dosimetry models, do not explicitly address how to adjust dosimetry to account for physiological and anatomical differences of young children. Instead the potential variability is believed to be addressed by UF applied for both database completeness and intrahuman variability. Thus, potential differences in delivered dose for children predicted by simulation studies such as those discussed in this session need to be evaluated in the context of determining the adequacy of these types of UF applied in most operational derivations to arrive at human health risk estimates.

Although limited in scope, the modeling approaches described in this paper may help inform considerations for adjusting existing RfC or deriving a life-stage specific RfC. Exactly how early life dosimetry differences that exist for one or several years are averaged over the longer lifetime to

which the RfC estimates apply may require a case-specific determination based on the critical effect. For example, as indicated by some of the analyses, there may be larger differences between deposition for some ages of children (e.g., infant to a 6-year old) than between other ages of children and adults (e.g., 12-year old and 21-year old). If unique windows of susceptibility for a specific disease coincide with those ages that also may receive higher doses, then a life stage specific RfC may be needed. The magnitude of the difference in dosimetry needs to be evaluated in context with that of the intrahuman UF and other UF that apply (e.g., database deficiencies). In contrast, if the relevant period of inhaled toxicant exposure is many years, then any higher dosimetry at an early life stage may need to be time-averaged with other age groups to adjust the RfC. In either case, it is important to document to what extent children's inhalation exposures have been considered when evaluating community exposures to inhaled toxicants.

The hierarchical model framework provided in the 1994 RfC methods (See Section 1 above) may be used to motivate new refinements that address age-specific considerations discussed in this manuscript. To implement such hierarchical considerations, suites of models were proposed to provide the flexibility to describe dose estimates with different levels of detail (Jarabek, 2000). The dose metric needs to be described at a level of detail that is commensurate with both the level of detail available regarding the toxic response and the intended duration of exposure for which the dose-response relationship is derived (U.S. EPA, 1994; Jarabek, 1995b). Thus, just as the preferred models for adults include species-specific and mechanistic determinants of chemical disposition and effect (Jarabek, 1995b; Bogdanffy and Jarabek, 1995), age-specific parameters and models such as those described in this session should be used. For example, in a given risk assessment the preferred model may take the form of a single-path mass transfer model to describe regional gas uptake (see Section 3 above), involve more refined multi-pathway deposition models (see Section 4 above), or be enhanced by chemical-specific information on reactions in the mucus layer (Section 5 above), metabolism in airway epithelium, and interaction with critical target molecules (e.g., the formaldehyde example in Section 6 above). All of these options should incorporate children's parameters to the extent possible.

DATA NEEDS

While techniques exist to develop a suite of modeling options, the limiting factor is having data of sufficient quality and reliability to support the required key parameters. The lack of age-specific anatomical and ventilation rate data is considered the key information gap. Additionally, the following are identified as data needs for children's inhalation dosimetry:

- A database able to support such a suite of models with sufficient sophistication and flexibility will require the compilation of an anatomical database for respiratory tract regions across a range of age groups (informed by imaging techniques, airway cast measurements, digital photographs of microscope slides or sectioned specimens, and scaling techniques).
- Age-specific clearance rates from respiratory regions.
- Breathing mode (normal augmentation versus mouth breathing), and the influence of ventilatory activity patterns on the relative contribution of nasal versus oral breathing, were shown to be key determinants of initial particle deposition and gas uptake (Snipes et al., 1997; Conolly et al., 2002).
- Determination of the switching point from nasal only to oral augmentation is likely to be different in children as discussed by Bennett et al. in a companion paper (Foos, et al.,2007); this will be an important consideration when using children's ventilation rate data.
- Physical attributes (e.g., particle size and distribution) and other physicochemical properties (e.g., composition and hygroscopicity) are also important and warrant characterization to refine models in both adults and children. For example, particle hygroscopicity influences inhaled deposition (ICRP, 1994; Schroeter et al., 2001).

Addressing these physicochemical, anatomical, and physiological data gaps will be key steps in building a suite of comprehensive dosimetry models for inhaled materials in both adults and children. Further, development of a comprehensive modeling capability across age groups may also decrease the reliance on default UF currently applied to account for intrahuman and database deficiencies.

DISCLAIMER

The views expressed in this paper are those of the authors and do not necessarily reflect the views or policies of the State of Connecticut or the U.S. Environmental Protection Agency. The U.S. Government has the right to retain a nonexclusive, royalty-free copyright covering this article.

ACKNOWLEDGMENTS

The preparation of this manuscript was supported by combined funding from USEPA Office of Children's Health Protection (OCHP) and USEPA, Office of Research and Development, National Center for Environmental Assessment, as part of the funding for the June 8–9, 2006 Children's Inhalation Workshop held in Washington, DC. In addition, research presented in Section 3 (default modeling

approaches) was supported by OCHP and the preparation of Section 6 (CFD modeling) was supported by funds provided by the American Chemistry Council (ACC) to the Chemical Industry Institute of Toxicology. The development of age-specific CFD models by scaling an adult model by children's nasal volumes was supported by the ACC and the U.S. Environmental Protection Agency conducted in collaboration with Ms. Annie Jarabek. The authors also wish to thank the peer review and insightful comments provided by Drs. Melvin Andersen, Linda Birnbaum, Harvey Clewell, Lynn Flowers, Gary Hatch, Elaina Kenyon, and Deirdre Murphy.

REFERENCES

Alcorn, J. and McNamara, P.J. 2002. Ontogeny of hepatic and renal systemic clearance pathways in infants. Part II. Clin Pharmacokinet. 41:1077–1094.

Andersen, M.E. and A.M. Jarabek. 2001. Nasal Tissue Dosimetry—Issues and Approaches for "Category 1" Gases: A report on a meeting held in Research Triangle Park, NC, 11–12 February, 1998. *Inhal. Toxicol. 13: 415–436*.

Andersen, M.E. and Sarangapani, R. 2001. Physiologically based clearance/extraction models for compounds metabolized in the nose: an example with methyl methacrylate. Inhal Toxicol. 13:397–414.

Andersen, M.E., Sarangapani, R., Frederick, C.B., and Kimbell, J.S. 1999. Dosimetric adjustment factors for methyl methacrylate derived from a steady-state analysis of a physiologically based clearance-extraction model. Inhal. Toxicol. 11:899–926.

Anjilvel, S., and Asgharian, B. 1995. A multiple-path model of particle deposition in the rat lung, *Fundam. Appl. Toxicol*. 28:41–50.

Asgharian, B., and Anjilvel, S. 1998. A multiple-path model of fiber deposition in the rat lung. *Toxicol. Sci.* 44:80–86.

Asgharian B., Hofmann W., and Bergmann R. 2001. Particle deposition in a multiple-path model of the human lung. *Aerosol Sci Technol.* 34:332–339.

Asgharian, B., Ménache, M.G., and Miller, F.J. 2004. Modeling Age-Related Particle Deposition in Humans, *J. Aerosol Med.* 17:213–224.

Bailey, M.R., Ansoborlo, E., Camner, P., Chazel, V., Fritsch, P., Hodgson, A., Kreyling, W.G., Le Gall, B., Newton, D., Paquet, F., Stradling, N., and Taylor, D. M. 2003. RBDATA-EULEP: Providing information to improve internal dosimetry. *Radiat. Protect. Dosimetry* 105:633–636.

Becquemin, M.H., Yu, C.P., Roy, M., Bouchikhi, A. and Teillac, A. 1991. Total deposition of inhaled particles related to age: comparison with age-dependent model calculations. Radiat. Prot. Dosimetry. 38:23–28.

Becquemin, M.H., Roy, M., Robeau, D., Bonnefous, S., Piechowski, J., and Teillac, A. 1987. Inhaled particle deposition and clearance from the normal respiratory tract. Respir Physiol. 67:147–158.

Beech D.J., Sibbons, P.D., Howard, C.V., and Van Velzen, D. 2000. Terminal bronchiolar duct ending number does not increase post-natally in normal infants. *Early Human Dev* 59:193–200.

Bennett, W.D. and Zeman, K.L. 1998. Deposition of fine particles in children spontaneously breathing at rest. Inhal. Toxicol. 10:831–842.

Berglund, D.J., Abbey, D.E., Lebowitz, M.D., Knutsen, S.F., and McDonnell, W.F. 1999. Respiratory symptoms and pulmonary function in an elderly nonsmoking population, *Chest* 115:49–59.

Beyer, U., Franke, K., Cyrys, J., Peters, A., Heinrich, J., Wichmann, H.E., and Brunekreef, B. 1998. Air polution and respiratory health of children: the PEACE panel study in Hettstedt and Zerbst, Eastern Germany, *Eur. Resp. Rev.* 8:61–69.

Bierbaum, S., and Heinzmann, A. 2007. The genetics of bronchial asthma in children. Respir. Med.101:1369–1375.

Bhalla, D.K.1999. Ozone-induced lung inflammation and mucosal barrier disruption: Toxicology, mechanisms and implications. J. Toxicol. Environ. Health Part B. 2:31–86.

Bobak, M. and Leon, D.A. 1999. The effect of air pollution and infant mortality appears specific for respiratory causes in the postneonatal period. Epidemiology 10:666–670.

Bogdanffy, M. S. and Jarabek, A. M. 1995. Understanding mechanisms of inhaled toxicants: implications for replacing default factors with chemical-specific data. *Toxicol. Lett.* 82/83:919–932.

Bogdanffy, M.S., Daston, G., Faustman, E.M., Kimmel, C.A., Kimmel, G.L., Seed, J., and Vu, V. 2001. Harmonization of cancer and noncancer risk assessment: Proceedings of a consensus-building workshop *Toxicol. Sci.* 61:18–31.

Bosma, J.F. 1986. *Anatomy of the Infant Head* The John Hopkins Univ. Press, Baltimore.

Bunge, M. 1987. Seven desiderata of rationality. In: *Rationality: The Critical View*, Ed. J. Agassi and I. Jarvie. Martinus Jijhoff Publishers, pp. 3.

Bush, M.L., Zhang, W., Ben-Jebria, A., and Ultman, J.S. 2000. Longitudinal distribution ozone and chlorine in the human respiratory tract: simulation of nasal and oral breathing with the single-path diffusion model. Toxicol. Appl. Pharmacol. 88:2015–2022.

Carey, S.A., Minard, K.R., Trease, L.L., Wagner, J.G., Garcia, G.J.M., Ballinger, C.A., Kimbell, J.S., Plopper, C.G., Corley, R.A., Postlethwait, E.M., and Harkema, J.R. 2007. Three-dimensional mapping of ozone-induced injury in the nasal airways of monkeys using nuclear magnetic resonance imaging and morphometric techniques. Toxicol. Pathol., in press.

Chang, L.Y., Huang, Y., Stockstill, B.L., Graham, J.A., Grose, E.C., Menache, M.G., Miller, F.J., Costa, D.L. and Crapo, J.D. 1992. Epithelial injury and interstitial fibrosis in the proximal alveolar regions of rats chronically exposed to a simulated pattern of urban ambient ozone. Toxicol Appl Pharmacol 115:241–252.

Charnock, E.L., and Doershuk, C.F. 1973. Developmental aspects of human lung, *Pediat. Clin. North Am.* 20:275–292.

Cheng, Y.S. 2003. Aerosol deposition in the extrathoracic region, *Aerosol Sci. Technol.* 37:689–671.

CIIT Centers for Health Research. Multiple-Path particle Dosimetry Model (MPPD). Version 2.0. Available on-line at: www.ciit.org.

Cohen Hubal, E.A., Kimbell, J.S., and Fedkiw, P.S. 1996. Incorporation of nasal-lining mass-transfer resistance into a CFD model for prediction of ozone dosimetry in the upper respiratory tract. Inhal. Toxicol. 8:831–857.

Cohen Hubal, E.A., Schlosser, P.M., Conolly, R.B., and Kimbell, J.S. 1997. Comparison of inhaled formaldehyde dosimetry predictions with DNA-protein cross-link measurements in the rat nasal passages. Toxicol. Appl. Pharmacol. 143:47–55.

Conceição, G.M.S., Miraglia, S.G.E., Kishi, H.S., Saldiva, P.H.N., and Singer, J.M. 2001. Air pollution and child mortality: a time-series study in São Paulo, Brazil, *Environ. Health Persp*. 109(Suppl. 3):347–350.

Conolly, R.B., Kimbell, J.S., Janszen, D.B., and Miller, F.J. 2002. Dose-response for formaldehyde-induced cytotoxicity in the human respiratory tract. Reg. Toxicol. Pharmacol. 35:32–43.

Conolly, R.B., Kimbell, J.S., Janszen, D.B., Schlosser, P.M., Kalisak, D.L., Preston, J., and Miller, F.J. 2004. Human respiratory tract cancer risks of inhaled formaldehyde: Dose-response predictions derived from biologically-motivated computational modeling of a combined rodent and human dataset. Toxicol. Sci. 82:279–296.

Conolly, R.B., Lilly, P.D., and Kimbell, J.S. 2000. Simulation modeling of the tissue disposition of formaldehyde to predict nasal DNA-protein cross-links in F344 rats, rhesus monkeys, and humans. Environ. Health Persp. 108(Suppl 5):919–924.

Corley, R.A., Minard, K.R., Einstein, D.R., Jacob, R.E., Kabilan, S., Trease, L.L., Hoffman, E.A., Postlethwait, E.M. Plopper, C.G., Kimbell, J.S., Harkema, J.R., Hlastala, M., and Timchalk, C. 2006. Advancements in modeling the respiratory system. Abstract No. 35. *2006 Itinerary Planner*. San Diego, CA: Soc. Toxicol.

Crawford-Brown, D.J. 2005. The concept of 'Sound Science' in risk management decisions. *Risk Manage,* **7**, 7–10.

Dahl, A.R, Schlesinger, R.B., Heck, H.d'A., Medinsky, M.A., Lucier, G.W. 1991 Comparative dosimetry of inhaled materials: Differences among animal species and extrapolation to man. *Fundam. Appl. Toxicol*. 16: 1–13.

Dunnill, M.S. 1962. Postnatal growth of the lung, *Thorax* 17:329–333.

Ferng, S.F., Castro, C.E., Afifi, A.A., Bermudez, E. and Mustafa, M.G. 1997. Ozone-induced DNA strand breaks in guinea pig tracheobronchial epithelial cells. J Toxicol Environ Health 51: 353–367.

Food Quality Protection Act (FQPA). 1996. Public Law 104–170, August 3, 1996. Available at http://www.epa.gov/pesticides/regulating/laws/fqpa/gpogate.pdf.

Foos, B., Marty, M., Schwartz, J., Bennett, W., Moya, J., Jarabek, A.M., and Salmon, A.J. 2007. Focusing on Children's Inhalation Dosimetry and Health Effects for Risk Assessment: an Introduction. J. Toxicol. Environ. Health, in press.

Frederick, C.B., Bush, M.L., Lomax, L.G., Black, K.A., Finch, L., Kimbell, J.S., Morgan, K.T., Subramaniam, R.P., Morris, J.B., and Ultman, J.S. 1998. Application of a hybrid computational fluid dynamics and physiologically-based inhalation model for interspecies dosimetry extrapolation of acidic vapors in the upper airways. Toxicol. Appl. Pharmacol. 152:211–231.

Gauderman, W.J., Gilliland, G.F., Vora, H., Avol, E., Stram, D., McConnell, R., Thomas, D., Lurmann, F., Margolis, H.G., Rappaport, E.B., Behane, K., and Peters, J.M. 2002. Association between air pollution and lung function growth in southern California children: results from a second cohort, *Am. J. Respir. Crit. Care Med.* 166:76–84.

Gent, J.F., Triche, E.W., Holford, T.R., Belanger, K., Bracken, M.B., Beckett, W.S. and Leaderer, B.P. 2003. Association of low level ozone and fine particles with respiratory symptoms in children with asthma. JAm.Med.Assoc. 290: 1859–1867.

Ginsberg, G.L., Foos, B.P., and Firestone, M.P. 2005. Review and analysis of inhalation dosimetry methods for application to children's risk assessment. J. Toxicol. Environ. Health (Part A). 68:573–615

Greim, H., Borm, P., Schins, R., Donaldson, K., Driscoll, K., Hartwig, A., Kuempel, E., Oberdörster, G., and Speit, G. 2001. Toxicity of fibers and particles — Report of the workshop held in Munich, Germany, 26–27 October 2000.

Grotberg, J.B., Sheth, B.V. and Mockros, LF. 1990. An analysis of pollutant gas transport and absorption in pulmonary airways. J. Biomech. Eng. 112: 168–176.

Guengerich, FP, Kim, DH and Iwasaki, M. 1991. Role of human cytochrome P-450 IIE1 in the oxidation of many low molecular weight cancer suspects. Chem Res Toxicol 4: 168–179.

Guilmette, R.A., Wicks, J.D., and Wolff, R.K. 1989. Morphometry of human nasal airways *in vivo* using magnetic resonance imaging, *J. Aerosol Med.* 2:365–377.

Ha, E-H., Lee, J-T, Kim, H., Hong, Y-C., Lee, B-E, Park, H-S. and Christiani, D.C. 2003. Infant susceptibility of mortality to air pollution in Seoul, South Korea. Pediatrics 111: 284–290.

Haefeli-Bleuer B. and Weibel, E.R. 1988. Morphometry of the human pulmonary acinus. *Anat. Rec.* 220:401–414.

Hanna, L.M., Lou, S-R., Su, S., and A.M. Jarabek. 2001. Mass Transport Analysis: Inhalation RfC Methods Framework for Interspecies Dosimetric Adjustment. *Inhal. Toxicol. 13: 437–463.*

Heyder, J., Armbruster, L., Gebhart, J., Grein, E., and Stahlhofen, W. 1975. Total deposition of aerosol particles in the human respiratory tract for nose and mouth breathing. J. Aerosol Sci 6: 311–328.

Hislop A. and Reid, L. 1974. Development of the acinus in the human lung. *Thorax.* 29:90–94.

Hislop A.A., Wigglesworth, J.S., and Desai, R. 1986. Alveolar development in the human fetus and infant. *Early Human Dev.* 13:1–11.

Horsfield K. and Cumming, G. 1968. Morphology of the bronchial tree in man. *J. Appl. Physiol.* 24:373–383.

Hotchkiss, J.A., Herrera, L.K., Harkema, J.R., Kimbell, J.S., Morgan, K.T., and Hatch, G.E. 1994. Regional differences in ozone-induced nasal epithelial cell proliferation in F344 rats: Comparison with computational mass flux predictions of ozone dosimetry. Inhal. Toxicol. 6(Suppl):390–392.

International Commission on Radiological Protection (ICRP). 1994. *Human Respiratory Tract Model for Radiological Protection*, Publication 66, Pergamon Press, Oxford, United Kingdom, Annals of ICRP. 24:272.

International Life Sciences Institute (ILSI). 2000. ILSI Risk Science Institute Workshop: The relevance of the rat lung response to particle overload for human risk assessment: A workshop consensus resport. *Inhal. Toxicol.* 12: 1–17.

Janssens, H.M, de Jongste, J.C., Fokkens, W.J., Robben, S.G., Wouters, K., and Tiddens, H.A. 2001. The Sophia anatomical infant nose-throat (SAINT) model: a valuable tool to study aerosol deposition in infants, *J. Aerosol Med.* 14:433–441.

Jarabek, A.M., Miller, F.J., and Asgharian, B. 2005. Dosimetric Adjustments for Interspecies Extrapolation of Inhaled Poorly Soluble Particles (PSP). *Inhal. Toxicol. 17:317–334.*

Jarabek, A.M. 1995a. The application of dosimetry models to identify key processes and parameters for default dose-response assessment approaches. *Toxicol. Lett. 79: 171–184.*

Jarabek, A. M. 1995b. Interspecies extrapolation based on mechanistic determinants of chemical disposition. *Human Ecol. Risk Assess.* 1:641–662.

Jarabek, A. M. 2000. Mode of action: Framework for dosimetry model development. Presented in: *Mode-of-Action Dosimetry: An Interagency Project to Develop Models for Inhalation, Oral, and Dermal Disposition.* Annual Meeting of the Society for Risk Analysis, 4–6 December, Arlington, VA. Abstract available online at: http://www.sra.org.

Jarabek, A.M. and Crawford-Brown, D.J. (*Personal communication).*

Kimbell, J.S. 2006. Nasal dosimetry of inhaled gases and particles: Where do inhaled agents go in the nose? Toxicol. Pathol. 34:270–273.

Kimbell, J.S., Schroeter, J.D., and Foureman, G.L. 2005a. Intrahuman variability in nasal dosimetry among four individuals. Final Program, Society for Risk Analysis Annual Meeting, Orlando, FL, December 4–7, 2005.

Kimbell, J.S., Kalisak, D.L., Conolly, R.B., Miller, F.J., and Jarabek, A.M. 2005b. A mechanistic model of lifetime cancer risk for inhalation exposures to reactive gases. Abstract 1304. The Toxicologist CD - An Official Journal of the Society of Toxicology, Volume 84, Number S-1, March 2005.

Kimbell, J.S., Gross, E.A., Richardson, R.B., Conolly, R.B., and Morgan. K.T. 1997. Correlation of regional formaldehyde flux predictions with the distribution of formaldehyde-induced squamous metaplasia in F344 rat nasal passages. Mutat. Res. 380:143–154.

Kimbell, J.S., Overton, J.H., Subramaniam, R.P., Schlosser, P.M., Morgan, K.T., Conolly, R.B., and Miller, F.J. 2001b. Dosimetry modeling of inhaled formaldehyde: Binning nasal flux predictions for quantitative risk assessment. Toxicol. Sci. 64:111–121.

Kimbell, J.S., Subramaniam, R.P., Gross, E.A., Schlosser, P.M., and Morgan, K.T. 2001a. Dosimetry modeling of inhaled formaldehyde: Comparisons of local flux predictions in the rat, monkey, and human nasal passages. Toxicol. Sci. 64:100–110.

Koblinger, L., and Hofmann, W. 1985. Analysis of human lung morphometric data for stochastic aerosol deposition calculations. *Phys. Med. Biol.* 30:541–556.

Koblinger, L., and Hofmann, W. 1990. Monte Carlo modeling of aerosol deposition in human lungs. Part I: simulation of particle transport in a stochastic lung structure. *J. Aerosol Sci.* 21: 661–674.

Landrigan, P. 1999. Risk assessment for children and other sensitive populations. Annals N.Y. Acad. Sci. 895: 1–9.

Makri, A., Goveia, M., Balbus, J. and Parkin, R. 2004. Children's susceptibility to chemicals: A review by developmental stage. J. Toxicol. Environ. Health Part B 7: 417–435.

Ménache, M.G., Hofmann, W., Ashgharian, B., and Miller, F.J. (Personal communication)

Miller F.J., Overton, J.H., Jaskot, R.H. and Menzel, D.B. 1985. A model of the regional uptake of gaseous pollutants in the lung. Toxicol. Appl. Pharmacol. 79:11–27.

Montgomery, W.M., Vig, P.S., Staab, E.V., and Matteson,S.R. 1979. Computed tomography: A three-dimensional study of the nasal airway, *Am. J. Orthodol.* 76:363–375.

Morgan, K.T. 1994. Nasal dosimetry, lesion distribution, and the toxicologic pathologist: a brief review. Inhal. Toxicol. 6 (Suppl): 41–57.

Mortensen, J.D., Schaap, R.N., Bagley, B., Stout, L., Young, J.D., Stout, A., Burkart, J.A., and Baker, C.D. 1983. Final report: *a study of age specific human respiratory morphometry*, Tech. Rep. TR 01525–010, University of Utah Research Institute, UBTL Division.

Moulin, F.J., Brenneman, K.A., Kimbell, J.S., and Dorman, D.C. 2002. Predicted regional flux of hydrogen sulfide correlates with distribution of nasal olfactory lesions in rats. Toxicol. Sci. 66:7–15.

National Council on Radiological Protection and Measurements (NCRP). 1997. Deposition, retention and dosimetry of inhaled radioactive substances, NCRP Report 125, Bethesda, MD.

National Research Council. 1994. Science and Judgment in Risk Assessment. National Academy Press. Washington, D.C.

Niinimaa, V., Cole, P., Mintz, S., and Shephard, R.J. 1981. Oronasal distribution of respiratory airflow. *Respir. Physiol.* **43,** 69–75.

Nodelman, V. and Ultman, J.S. 1999. Longitudinal distribution of chlorine absorption in human airways: comparison of nasal and oral quiet breathing. J. Appl. Physiol. 86: 1984–1993.

Nong, A., McCarver, D.G., Hines, R.N. and Krishnan, K. 2006. Modeling interchild differences in pharmacokinetics on the basis of subject-specific data on physiology and hepatic CYP2E1 levels: a case study with toluene. Toxicol Appl Pharmacol 214: 78–87.

Oberdörster, G., Ferin, J., and Lehnert, B.E. 1994. Correlation between particle size, *in vivo* particle persistence, and lung injury. *Environ. Health Persp.* 102(Suppl 5):173–179.

Overton, J.H. 2001. Dosimetry modeling of highly soluble reactive gases in the respiratory tract. *Inhal. Toxicol.* 13: 347–357.

Overton, J.H., and Graham, R.C. 1989. Predictions of ozone absorption in human lungs from newborn to adults, *Health Physics* 57(Suppl. 1):29–36.

Overton JH, Graham RC, Miller FJ. 1987.A model of the regional uptake of gaseous pollutants in the lung. II. The sensitivity of ozone uptake in laboratory animal lungs to anatomical and ventilatory parameters. *Toxicol. Appl. Pharmacol.* 88: 418–32.

Overton, J.H., Kimbell, J.S., and Miller, F.J. 2001. Dosimetry modeling of inhaled formaldehyde: The human respiratory tract. Toxicol. Sci. 64:122:134.

Pinkerton, K.E., Green, F.H.Y., Saike, C., Vallyathan, V., Plopper, C.G., Gopal, V., Hung, D., Bahne, E.B., Lin, S.S., Ménache, M.G., and Schenker, M.B. 2000. Distribution of particulate matter and tissue remodeling in the human lung. *Environ. Health Persp.* 108:1063–1069.

Phalen, R.F., Oldham, M.J., Beaucage, C.B., Crocker, T.T., and Mortensen, J.D. 1985. Postnatal enlargement of human tracheobronchial airways and implications for particle deposition, *Anat. Rec.* 212:368–380.

Raabe, O.G., Al-Bayati, M.A., Teague, S.V., and Rasolt, A. 1988. Regional deposition of inhaled monodisperse, coarse, and fine aerosol particles in small laboratory animals. In: Dodgson, J; McCallum, RI; Bailey, MR; Fischer, DR., Eds. *Inhaled Particles VI: Proceedings of an International Symposium and Workshop on Lung Dosimetry*; September, 1985; Cambridge, United Kingdom. *Ann. Occup. Hyg.* 32 (Suppl. 1): 53–63.

Reid, L. 1984. Lung growth in health and disease, *Br. J. Dis. Chest* 78: 113–134.

Robinson, R.J. and Yu, C.P. 2001. Deposition of cigarette smoke particles in the human respiratory tract, *Aerosol Sci. Technol.* 34:202–215.

Rudolf, G., Kobrich, R., and Stahlofen, W. 1990. Modeling and algebratic formulation of regional aerosol deposition in man. *J. Aerosol Sci.* 21(Suppl. 1.):S403-S406.

Rudolf, G., Gebhart, J., Heyder, J., Schiller, Ch.F., Stahlhofen, W. 1986. An empirical formula describing aerosol deposition in man for any particle size. *J. Aerosol Sci.* 17:350–355.

Santiago, L.Y., Hann, M.C., Ben-Jebria, A., and Ultman, J.S. 2001. Ozone absorption in the human nose during unidirectional airflow. *J. Appl. Physiol.* 91:725–732.

Sarangapani, R., Gentry, P.R., Covington, T.R., Teeguarden, J.G., Clewell, H.J. 2003. Evaluation of the potential impact of age- and gender-specific lung morphology and ventilation rate on the dosimetry of vapors. Inhal. Toxicol. 15: 987–1016.

Schiller-Scotland, C.F., Hlawa, R., and Gebhart, J. 1994. Experimental data for total deposition in the respiratory tract of children. Toxicol. Lett. 72: 137–144.

Schroeter, J. D., Musante, C. J., Hwang, D., Burton, R., Guilmette, R., and Martonen, T. B. 2001. Hygroscopic growth and deposition of inhaled secondary cigarette smoke in human nasal pathways. *Aerosol Sci. Technol.* 34:137–143.

Schroeter, J.D., Kimbell, J.S., Andersen, M.E., and Dorman, D.C. 2006b. Use of a pharmacokinetic-driven computational fluid dynamics model to predict nasal extraction of hydrogen sulfide in rats and humans. Toxicol. Sci., 94:359–367.

Schroeter, J.D., Kimbell, J.S., Bonner, A.M., Roberts, K.C., Andersen, M.E., and Dorman, D.C. 2006a. Incorporation of tissue reaction kinetics in a computational fluid dynamics model for nasal extraction of inhaled hydrogen sulfide in rats. Toxicol. Sci. 90: 198–207.

Schwartz, J. 2004. Air pollution and children's health. Pediatrics 113: 1037–1043.

Segal, R.A., Kepler, G.M., and Kimbell, J.S. 2004. Correlation of nasal surface-area-to-volume ratio with predicted inhaled gas uptake efficiency in humans. Toxicol. Sci. 78(1-S), Abstract No. 2107. *2004 Itinerary Planner*. Baltimore, MD: Soc. Toxicol.

Snipes, M.B.; James, A.C.; Jarabek, A.M. 1997. The 1994 ICRP66 Human respiratory tract model as a tool for predicting lung burdens from exposures to environmental aerosols. *Appl. Occup. Environ. Hyg.* 12: 547–554.

Sonnier, M. and Cresteil, T. 1998. Delayed ontogenesis of CYP1A2 in the human liver. Eur. J. Biochem. 251: 893–898.

Swift, D.L. 1991. Inspiratory inertial deposition of aerosols in human nasal airway replicate casts: Implications for the proposed NCRP lung model, *Rad. Prot. Dosimetry*. 38:29–44.

Swift, D.L., Cheng, Y.-S., Su, Y.-F., and Yeh, H.-C. 1994. Ultrafine aerosol deposition in the human nasal and oral passages, *Ann. Occup. Hyg.* 38(Suppl. 1):77–81.

Thurlbeck, W.M. 1988. Quantitative anatomy of the lung. In: Thurlbeck WM, ed. *Pathology of the Lung.* Stuttgart: Thieme, pp.51–55.

Treybal, R.E. 1980. "Mass-Transfer Operations." McGraw-Hill, New York, 3rd edition. pp 70–77 & 106–111.

U.S. EPA. (U.S. Environmental Protection Agency). 1994. Methods for derivation of inhalation reference concentrations and application of inhalation dosimetry. EPA/600/8–90/066F.

U.S. EPA. (U.S. Environmental Protection Agency). 1996. Dosimetry of Inhaled Particles in the Respiratory Tract (Chapter 10). *Air Quality Criteria for Particulate Matter. Volume II of III*. Office of Research and Development, Washington, DC. EPA/600/P-95/001bF. April.

U.S. EPA. (U.S. Environmental Protection Agency). 2002. Child-Specific Exposure Factors Handbook. EPA-600-P-00–002B.

U.S. EPA. (U.S. Environmental Protection Agency). 2004. Dosimetry of Particulate Matter (Chapter 6). *Air Quality Criteria for Particulate Matter. Volume II of II.* Office of Research and Development, Washington, DC. EPA 600P-99/002bF.

U.S. EPA. (U.S. Environmental Protection Agency). 2005. *Guidelines for Carcinogen Risk Assessment*. Risk Assessment Forum, Office of Research and Development. Washington, DC. EPA/630/P-30/001F. March.

U.S. Environmental Protection Agency. 2006. Revision of the Metabolically-Derived Ventilation Rates within the Exposure Factors handbook. External Review Draft. Office of Research and Development, Washington, D.C. EPA/600/R-06/129A. http://cfpub.epa.gov/ncea/cfm/recordisplay.cfm? deid=160065

Vieira, I., Sonnier, M. and Cresteil, T. 1996. Developmental expression of CYP2E1 in the human liver. Hypermethylation control of gene expression during the neonatal period. Eur J Biochem 238:476–483.

Weibel, E.R. 1963. *Morphometry of the Human Lung*, Springer Verlag, Berlin.

Wolff, R.K. Mucociliary function. In: Parent RA, ed. Comparative biology of the normal lung. Ann Arbor:CRC Press, 1992. pp 659–680.

Xu, G.B., and Yu, C.P. 1986. Effects of age on deposition of inhaled aerosols in the human lung, *Aerosol Sci. Technol*. 5:349–357.

Yeh H.C. and Schum, G.M. 1980. Models of human lung airways and their application to inhaled particle deposition. *Bull. Math. Biol.* 42:461–480.

Yu, C.P. 1978. Exact analysis of aerosol deposition during steady breathing. *Powder Technol*. 21:55–62.

Yu, C.P., and Xu, G.B. 1987. Predicted deposition of diesel particles in young humans, *J. Aerosol Sci.* 18:419–429.